9. Geophysical and archaeological surveys: methods and results

9.1. Geophysical and archaeological surveys in Nessonis 1: a synopsis

Agathe Reingruber, Giorgos Toufexis, Grigorios Tsokas, Alexandros Stampolidis, Nikolaos Kordatos, Spyridon Maroulakis and Amelie Mohrs

9.1.1. The location of the flat site Nessonis 1-South

In December 2020, the flat site of Nessonis 1-South (NES1-S), fields F013–F015 and F400–401, has been investigated geophysically based on the results from the archaeological prospections. NES1-S is a flat site of the Early Neolithic and is located directly south of the Magoula Nessonis 2 (NES2). In this area only little modern interventions are observable and no modern constructions have been erected. Heavy machinery is not being used for cultivation, and deep ploughing is not common. The most pronounced intrusions relate to the planting and irrigation of almond groves: for the single trees 50–60 cm deep holes have to be sunken into the soil and for their irrigation metal pipes are used. These have a clearly negative effect on the geophysical evaluation.

This flat area is among the lowest parts in the basin of Sykourio, just below 87 masl (some smaller depressions are located at 85 masl). It is bordered by the Chassambali hills in the south and the former Lake Bara Toibasi in the northeast (Figs. 9.1.1–2). Both their assets have been used during the last century either for road constructions (serpentinite from the hills) or for tiles (fine clays from the lake sediments) – this explains the heavily overworked parts east of NES1-S, an area where Nessonis 1-East (NES1-E) must have been located before destruction.[1]

In five of the investigated fields pottery and small finds of the EN II–III lay especially close to the pits dug for the planting of the almond trees and were brought to light during this horticultural work. Between the fields small ridges are visible outlining their borders with piled up stones and debris (Fig. 9.1.3). East and west of these five fields no prehistoric finds were revealed (e.g. in TOI-F8 or TOI-F14, -F18, compare Ch. 2, Fig. 2.7). Farther east, south of the clay extraction pits where NES1-E should have been positioned, the soil is heavily worked up in modern times and the visibility is very low (Figs. 9.1.1–2). The site ends in the south of fields F013, F014 and F013A at the foothills of the Chassambali. In the north, a dirt road separates it from the Magoula NES2.

9.1.2. Magnetic gradiometry and susceptibility measurements in Nessonis 1

It is well known that magnetic survey is the geophysical method most frequently employed for the investigations at archaeological sites.[2] Some information about the method and the merit of using two sensors separated by a small vertical distance (gradient mode) can be found in this same volume (contribution by Tsokas et al., Chapter 9.2).

In the case of Nessonis, the optically pumped Cesium magnetometer was used in the gradient mode. This is an instrument based on the so-called Zeeman's phaenomenon, i.e. to the split up of the spectral lines of the atoms of the Alkalis at the presence of magnetic field.

Figure 9.1.4 shows the instrument in action in Nessonis. The particular unit is the G-858 gradiometer of Geometrics, Inc.

The receiver of a differential GPS was mounted to the gradiometer cart neglecting the need to

[1] NES1-E, formerly Nessonis I, located 200 m east of NES2, was first mentioned and investigated by D. Theocharis with a small sounding (Theocharis 1962). It was not located again by Gallis (1992) and also our search was unsuccessful in this heavily disturbed area. NES1-S was discovered during the survey project in 2017, and in order to retain the numbering suggested by Theocharis, we decided to name it accordingly.

[2] Gaffney 2008; Fassbinder 2015; Herbich 2015.

Publiziert in: Reingruber, Agathe; Toufexis, Giorgos (Hg.): Siedlungsdynamik in den Becken von Sykourio und Elateia, Nordost-Thessalien, in prähistorischer Zeit. Ergebnisse der archäologischen, geomorphologischen und geophysikalischen Untersuchungen, Heidelberg, Propylaeum, 2025 (Prähistorische Archäologie in Südosteuropa, Bd. 34). DOI https://doi.org/10.11588/propylaeum.1583

Fig. 9.1.1. Landscape east of Nessonis 1-South and Nessonis 2 with serpentinite outcrops in the fore- and clay extraction pits in the background (photo A. Reingruber).

Fig. 9.1.2. Nessonis 1-South and Nessonis 2 with grids from geophysical investigations.

establish grids on the ground surface. The other receiver (base) was put on the roof of the small hut housing water pumping gear which is very close to the surveyed area. Measurements were carried out along profiles roughly 0.5 m apart one from the other. The in line measuring step was about 0.05 m.

Processing of the data of the multisensory system involved the following modules:

- Removing outliers (abnormally low or high readings relative to their neighboring ones).
- Micro leveling: i.e., the application of 1D and 2D median filtering similar to the treatment of aeromagnetic data.
- Resampling to create the final 0.25 m x 0.25 m grid.
- Upward continuation by 0.25 m to diminish the high frequency noise.
- Next processing continued by using the same modules as for the single instrument survey. In fact, the modules of the sequence mentioned earlier were applied after the low pass filtering.

Fig. 9.1.3. Nessonis 1-South as seen from the north: Fields F014–F015 in the centre and F400 in the almond grove to the left (photo A. Reingruber).

- Compression of the dynamic range using the Arctan function.
- High pass filtering.
- Interpolation twice both in the X and Y direction using cubic splines of the form sinX/X[3].
- Application of Wallis filter[4].

Complementary to the magnetic prospection, measurements of the magnetic susceptibility of the topsoil and stones included therein – be them natural or deriving from prehistoric masonry (Table 9.1.1) – were carried out. The SM 30 ZH-Instruments susceptibility meter (or kappa-meter) was used. The particular instrument has been designed for field use and measures the so-called apparent susceptibility by connecting the unit to the material to be measured. It is well known that the readings provide an estimate of the concentration of ferrimagnetic minerals in the sampled volume. This is a rough measure to enhance the signals of magnetic minerals in the prehistoric settlement and its surroundings.[5]

The magnetic susceptibility readings are shown in Table 9.1.1. They demonstrate that the metamorphic rocks or conglomerates consisting of metamorphic cobbles as is the case of the Chassambali ophiocalcite (compare contribution by Vasilios Melfos, Chapter 5) possess a very large susceptibility contrast with the topsoil as well as with the calcitic material and sandstone. This means that the subsurface remnants of stone structures (foundations, piles, enclosures) would much likely show a pronounced positive magnetic effect.

Fig. 9.1.4. Measuring at Nessonis 1 with the G-858 Cs Magnetometer of Geometrics, Inc. (photo G. Tsokas).

[3] Scollar et al. 1986.
[4] Scollar et al. 1986.
[5] Tite and Mullins 1971.

9.1.3. A synopsis of the archaeological and geophysical investigations

The magnetogram of the site NES1-S shows a plenitude of signals (Fig. 9.1.5). As expected, the borders between fields marked by stones and also the metal pipelines for watering the almond trees make their presence noticeable as linear anomalies. Also the serpentinites from the hill dominate the magnetogram especially in the southern part. They complicate the detection and interpretation of the potentially prehistoric anomalies enormously (Fig. 9.1.6).

Nevertheless, some conspicuous features can be highlighted: The magnetogram is in the northeast, around the contour line at 87 masl, rather empty, containing mainly dipoles deriving from modern metals. In this area of field F401, the few small finds occurred only at its western limits and additionally sherds were few and often eroded (compare Chapter 6.2.1).

This situation may or may not have something to do with the (artificial/natural?) stripe that is running parallel to the 87 m contour line between F400 and F401. The prehistoric finds are located west of this stripe, and also the magnetic signals are more abundant here. Such separations between fields are visible in lines of signals running vertically or horizontally (Fig. 9.1.6, light grey) and are indicative of possible field-borders piled together from stones and debris. Between them, anomalies occur that may be related to prehistoric events since in these areas prehistoric finds abound.

In the southern part, among the strong signals from the serpentinites, some possibly prehistoric features can be filtered out. Outstanding are three almost rectangular anomalies, two oriented NW–SE (also at the site of Elateia 1 such rectangular anomalies were detected – compare Chapter 9.3). Their sizes vary between 8.3 x 4.5 m, 7 x 4.5 m and 5.8 x 4 m (Fig. 9.1.6, red squares) and are interpreted here provisionally as contours of constructions in which fire was handled (fireplaces, ovens) or which have been damaged by fire.

Some smaller roundish anomalies may derive from re-filled pits and working places with outdoor hearths. Such agglomerations are seen in the NW and possibly also in the central part. More difficult to be detected as archaeological anomalies are the roundish signals in the south, since they are intermingled with the amorphous irregular signals. These southern fields F013 and F014 are a bit higher up at 88–89 masl – here most of the decorated sherds were registered (Fig. 9.1.7) that we associate with domestic spheres.

Material	No. of samples	Mean apparent susceptibility SI x 10-3
Topsoil	12	2.323
Calcitic materials	5	0.0165
Sandstone	5	0.0655
Metamorphic	3	44.5

Table 9.1.1. Apparent magnetic susceptibility readings in the area of the magnetic survey in Nessonis 1.

When overlaying the magnetogram with the position of small finds measured with handheld GPS-devices, none of them directly cover one of the three rectangular signals (Fig. 9.1.8). At first sight the finds seem to spread quite evenly over the whole area, but heatmaps obtained for the different categories of finds according to materials and shapes show that there are several concentrations:

- small finds related to dwellings like decorated sherds, clay objects, a shell spoon, are occurring in the southern, the higher part of field F013 (Fig. 9.1.9).
- different kinds of grinding tools are found in the west in F014 and in F015 (Fig. 9.1.10).
- it is most interesting to observe that almost all chipped stone artefacts have been found in F400 in the lowest part of the site with only few distinguishable signals (Fig. 9.1.11).

9.1.4. An attempt at interpreting the site

Although the magnetogram is difficult to interpret, some observations can be suggested together with the evaluation of the finds. Equally important in this analysis are the contour lines and the exact heights of the features and finds. Just east and west of the 87 m contour line an area conspiciously empty of both signals and finds is acknowledgeable. Most finds occur between 87 and 88 masl, especially those related to harvesting and food processing. In contrast, around and above the 88 masl contour line three rectangular anomalies occur: one close to 88 masl, one above 88 masl and one above 89 masl. Pottery evaluation has shown that all sherds found in this southeastern field F013

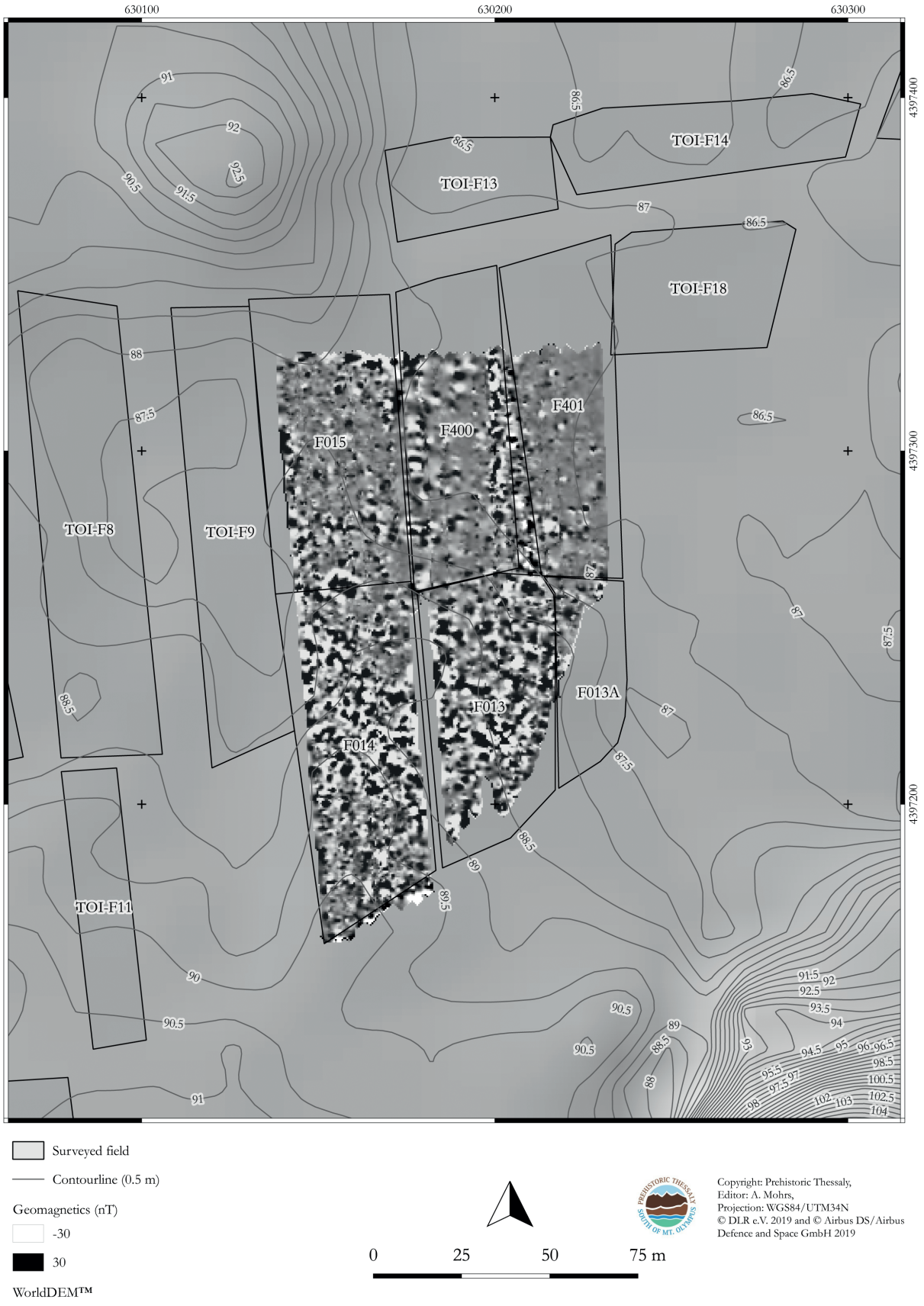

Fig. 9.1.5. Magnetogram of Nessonis 1-South with surveyed fields and contour lines at 0.5 m interval.

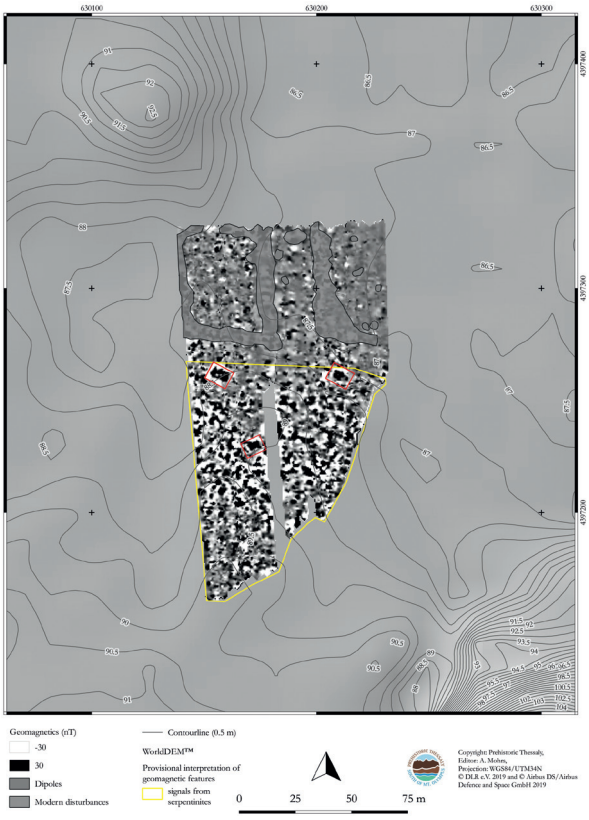

Fig. 9.1.6. Magnetogram of Nessonis 1-South with possible above ground constructions (red squares).

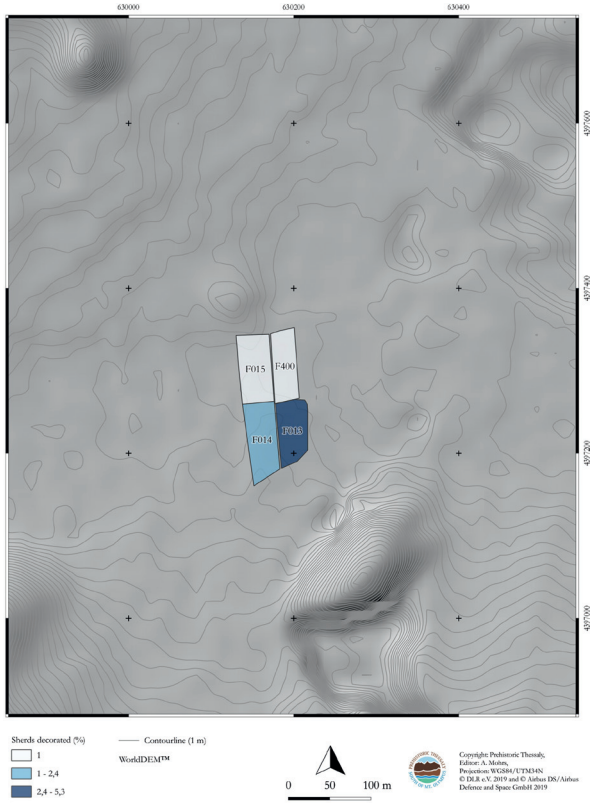

Fig. 9.1.7. Distribution of decorated sherds.

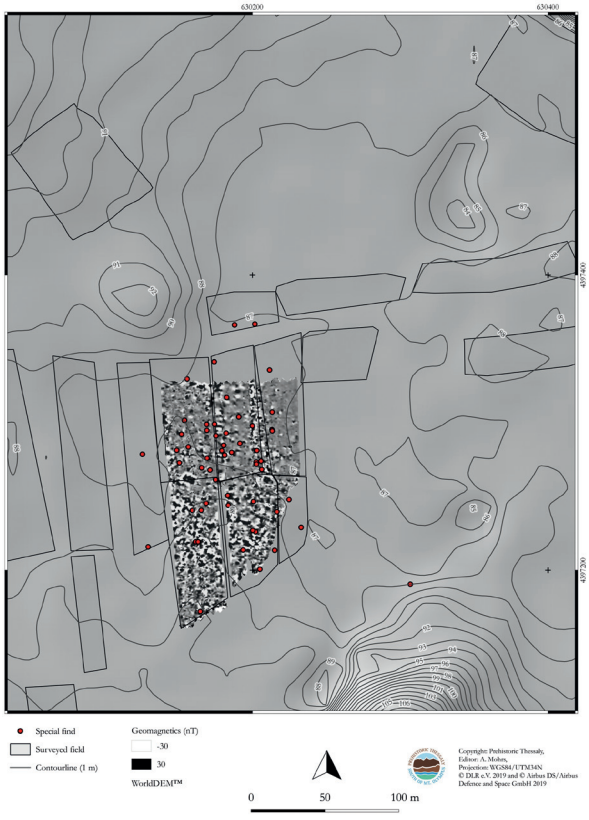

◄ Fig. 9.1.8. Small finds recorded three-dimensionally with handheld GPS-devices within the surveyed fields.

(early painted and blacktopped) can be securely dated into the EN II (Chapter 6.2.1, and Taf. 1). Decorative elements of the EN III/MN I (e.g. impressed pottery) appear in F014 and F015, west of F013. Also, vessel shapes that would best fit into the EN III/MN I occur rather in fields F014–F015 and F400 (Chapter 6.2.1, Taf. 2–3). Not a single decorated piece has been found in F400: this area is interpreted as an open space, used probably for gardening – and here also the chipped stones agglomerate. The space with ground stone tools west of the open area and just north of the rectangular anomaly F014/F015, may have been used for food preparation or cooking.

In the end, a horizontal shift from east to west may be suggested from the EN II to the EN III, from just around 88 masl to above 88 masl and 89 masl. Whereas the higher southern part was rather used for

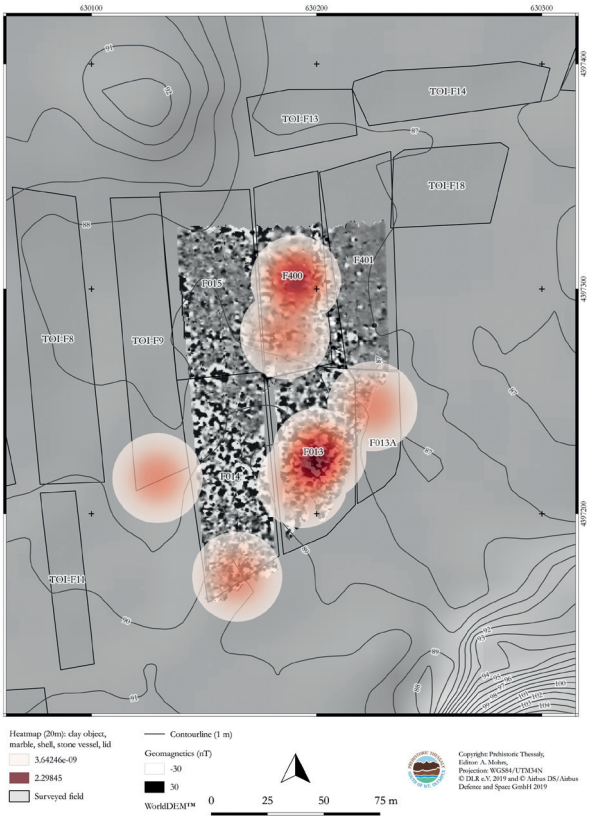

Fig. 9.1.9. Heatmap with special objects.

Fig. 9.1.10. Heatmap with grinding stones.

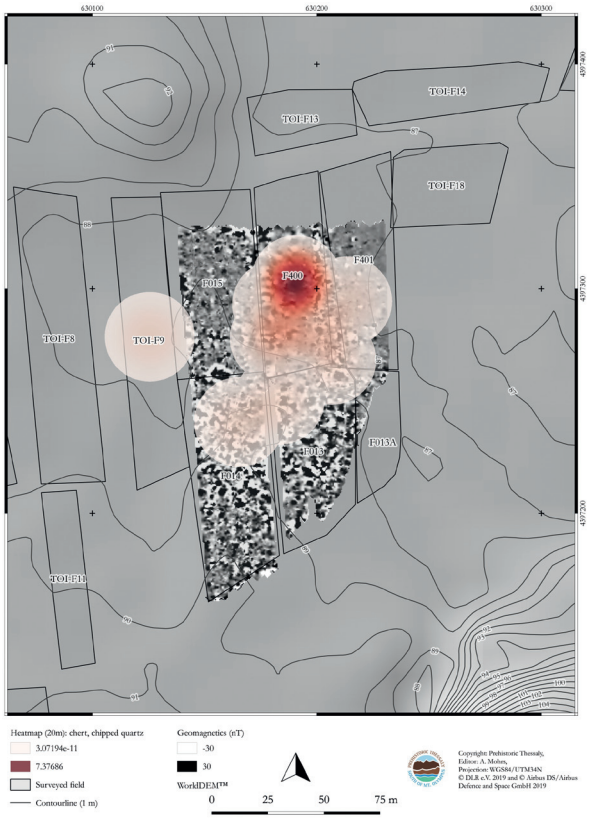

◄ Fig. 9.1.11. Heatmap with chipped stones.

living, in the lower northern part (between 87 and 88 masl) food production and processing took place.

Bibliography

Gaffney 2008: C. Gaffney, Detecting trends in the prediction of the buried past: a review of geophysical techniques in Archaeology. Archaeometry, 50(2), 2008, 313–336.

Fassbinder 2015: W.E.J. Fassbinder, Seeing beneath the farmland, steppe and desert soil: magnetic prospecting and soil magnetism. Journal of Archaeological Science 56, 2015, 85–95.

Herbich 2015: T. Herbich, Magnetic prospecting in archaeological research: a historical outline. Archaeologia Polona 53, 2015, 21–68.

Scollar et al. 1986: I. Scollar, B. Weidner and K. Segeth, Display of archaeological magnetic data. Geophysics, 51(3), 1986, 623–633.

Tite and Mullins 1971: M. S. Tite and C. Mullins, Enhancement of the magnetic susceptibility of soils on Archaeological sites. Archaeometry, 13(2), 1971, 209–219.

9.2. Geophysical survey at the Neolithic site of Elateia 1

Grigorios N. Tsokas(1), Alexandros Stampolidis(1), Agathe Reingruber(2), Giorgos Toufexis(3), Angelos Albanis(1), Prodromos Louvaris(1), Nikolaos Kordatos(1), Ilias Fikos(1), and Nikos Papadopoulos(4)

(1) Exploration Geophysics Laboratory, Aristotle University, Thessaloniki
(2) Institut für Prähistorische Archäologie, Freie Universität Berlin
(3) Ephorate for Antiquities, Larisa
(4) Laboratory of Geophysical-Satellite Remote Sensing and Archaeoenvironment, Rethymno

9.2.1. Introduction

The aim of this paper is to present the conduct, the data processing and the results of the magnetic survey carried out between October 2017 and December 2019 at the Neolithic site of Elateia in Thessaly. Also, in a second step emphasis is put on the interpretation of the obtained magnetograms which showed several anomaly patterns. Hence, we attempted to recognize patterns which could be attributed to buried features associated with the Neolithic occupation of the land. Their interpretation in connection with the results of the systematic archaeological prospections is discussed in more detail in Chapter 6.3 of this volume.
The survey was carried out using both single and multisensor modes because the site was partially covered by alleys of almond trees. The latter required the use of a single sensor in the alleys since it was impossible to move a multisensory cart in between the trees.

9.2.2. Measurements of the earth's magnetic field and magnetic gradiometry

Magnetometry constitutes the most frequently employed method for the investigation of the subsurface at archaeological sites.[1] Its operating principle consists of detecting rather weak and spatially restricted magnetic signals originated from buried remnants of past human activity. Its success relies on the fact that "worldwide almost all soils exhibit an enhancement of magnetic susceptibility in the top soils"[2]. This property of the soils was recognised already at the onset of the magnetic prospecting for archeological purposes,[3] whereas, besides the aforementioned studies, many others followed aiming to investigate the origin of such behavior.[4] It was also very early recognised that the magnetic susceptibility for the cultural soil layers was continuously enhanced.[5]
Though the surveying technique remains almost unaltered since the early days of the pioneers[6], instrumentation has been substantially evolved[7], carts were introduced for swift and dense areal coverage[8] and the instrumental precision has been enormously increased[9]. Further, the use of GPS has enhanced the positioning accuracy almost to the state of perfection for the purposes of archeological prospection. However, although nowadays the scale of magnetic surveys is very large, the majority of data was collected by using handheld single sensors.[10] In this study, the earth's magnetic field was partially recorded using a single fluxgate differential magnetometer whereas a battery of similar instruments covered another part of the area.
If two magnetic sensors are used to record the earth's field at two different height levels, their difference is an approximation of the vertical gradient of the field. In strict physical terms, it is an approximation of the the first vertical difference and, divided by the height difference, yields the approximation of the gradient. This mode of measuring the

1 Gaffney 2008.
2 Fassbinder 2015.
3 Le Borgne 1955, 1960; Mullins 1977.
4 Maher and Taylor 1988; Fassbinder et al. 1990; Fassbinder and Stanjek 1993; Fassbinder 2015.
5 Tite and Mullins 1971.
6 Aitken 1974.
7 Becker 1995; Linford 2006; Aspinall et al. 2008.
8 Neubauer et al. 1999; Becker 2001; Trinks et al. 2014, Rassmann et al. 2016.
9 Becker 1995; Linford et al. 2007.
10 Gaffney 2008.

earth's field is operationally advantageous since no correction is needed for its diurnal variation. Therefore, it has become very popular in archaeological prospection, where large numbers of measurements are necessary to sample densely the spatial variation of the field.

Magnetic prospecting yields an image of the spatial distribution of the magnetic field (magnetogram), in which the anomalous parts are indicative of buried magnetic structures. Positive anomalies reflect the presence of features more magnetic than the environment they are hosted in, whereas the negative ones reveal the presence of less magnetic features. The method can detect the anomalies created by strongly magnetized structures such as kilns, ovens, hearths, and in general features containing a large amount of burnt clay. On the other hand, it can also detect features such as ditches, pits, trenches, wall foundations and in general buried architectural remains, tombs, etc., which generate rather weak magnetic signals. Data processing has been also considerably developed.[11] In this respect, the objective of any archaeological prospection survey as set by I. Scollar and his team[12] is easily achieved, i.e. to have a final image that resembles the ground view of the buried ancient remains.

9.2.3. Magnetic surveys at Elateia 1 and data processing

Square cells were established on the ground surface in the area to be surveyed using a single instrument. These cells were 20 m x 20 m in size, in order to cope better with terrain irregularities and the alleys of the almond trees. In each cell, a 0.5 m x 0.5 m grid was created with measuring tapes. Magnetic measurements were taken with a gradiometer at 0.25 m intervals along traverses spaced 0.5 m apart from each other. In the present study, the FM256 Fluxgate gradiometer[13] of GEOSCAN RESEARCH was used. This is shown in Figure 9.2.1 along members of the field crew, during the measurements at Elateia. This instrument measures the first vertical difference of the vertical component of the magnetic field.

Variations in orientation and the zeroing of the instrument were checked regularly after the completion of each four grid squares. The data was downloaded onto a laptop in the field each time eight grid squares had been measured. This approach enabled a quick data-quality check *in situ.* Additional checks of the data as well as a first processing were performed at the end of each day of fieldwork. After the completion of the survey, data processing continued at the Laboratory of Exploration Geophysics at the Aristotelian University of Thessaloniki. The processing sequence was decided after various tests and included the following steps:

- Statistical analysis of the data.
- Transfer of the mean of each traverse to zero (Zero Mean Traverse).
- Despiking by median filter which was performed in 3X3 windows of the data.
- Low pass filtering.
- Interpolation both in the X and Y direction using cubic splines of the form sinX/X[14.] This processing step was applied twice.
- Application of Wallis filter[15].
- Creation of gray scale images in order to have the result in a form which resembles the result that would have been pictured if excavation had taken place.[16]
- Georeferencing of the arbitrary local coordinate system of the mesh of the cells to the Greek Geodetic Reference System (1987).

Part of the readings were taken using a battery of eight differential magnetometers mounted on a cart, which was also equipped with a controlling and logging unit. In this case positioning was done by employing a differential GPS whose antenna was mounted also on the cart. A second antenna was in operation at a stable position close to the area to be surveyed. The SENSYS MX V3 ensemble was employed for the survey. The magnetometers were placed at 0.5 m intervals whereas the in-line

[11] Stampolidis and Tsokas 2012; Eppelbaum 2014; Karamitrou et al. 2017.
[12] Scollar et al. 1986.
[13] Parasnis 1997.
[14] Scollar et. al. 1986.
[15] Scollar et. al. 1986.
[16] Scollar et. al. 1986.

Figure 9.2.1. Members of the field team during the data acquisition process at the Neolithic site of Elateia (photo G. Tsokas).

Figure 9.2.2. The cart with the fluxgate gradiometers, the control and log unit and the GPR antennae mounted during the field work in Elateia (photo G. Tsokas).

measuring interval was approximately 0.05 m and the whole cart was moving back and forth on the fields in a zigzag mode. A back up of the data was performed in regular time intervals. After the completion of the survey, processing and visualisation was performed in the Lab. Figure 9.2.2 shows the cart with the battery of the magnetometers in action in Elateia.

Processing of the data of the multisensory system involved the following modules:

- Editing to remove erratic reading resulting from irregular movements of the cart, etc.
- Zeroing of the mean of the readings along the individual traverses.
- Micro levelling: i.e. the application of 1D and 2D median filtering similar to the treatment of aeromagnetic data.
- Resampling to create the final 0.25 m x 0.25 m grid.
- Upward continuation by 0.25 m to diminish the high frequency noise. Note that 0.25 m is the unit spacing of the final grid.
- Further processing continued using the same modules as for the single instrument survey. In fact, the modules of the sequence mentioned earlier after the low pass filtering were applied.

9.2.4. Discussion of the results of magnetic mapping

In order to better highlight anomalies of interest (Figure 9.2.3), the so-called tilt angle transformation[17] of the data was computed and presented in Figure 9.2.4.

The dominant feature in the magnetograms is the semicircular anomaly extending all over the northern and north-eastern parts. This is very clearly seen and presumably reflects the presence of a ditch, concealed by the soil cover. Ditches are very often found at the Neolithic sites and they could have been dug for various reasons. In the present case, it seems that it served as an anti-flooding measure to prevent the water of the nearby creek to damage the village (for a more detailed interpretation compare Chapter 9.3).

Another, positive elongated anomaly shows up at the eastern part of the magnetogram: it leads from the arc of the anomaly (the outer ditch) in a straight line into the interior of the settlement and towards another linear anomaly. We interpret it as a secondary ditch.

An elongated anomaly curving gently at the central western part of the magnetogram is located at distances ranging between 70 and 130 m from the main ditch discussed previously. This could be attributed to the presence of some other internal secondary ditch or enclosure. However, we cannot exclude that this anomaly may be the result of the shifting surface. Similarly, another linear anomaly in NW–SE direction, located southwards of the former one, may have the same origin i.e. that of a land slide. Given the topography of the site (compare Figs. 6.33 and 6.43), the highest area is in the eastern central part where the outer ditch iends in the almond grove. Therefore, it is rather the linear or slightly curved extended anomalies in the southern and western part that could have a natural origin.

A relatively strong anomaly appears in the central part, consisting of several linear sections that yield a shape reminiscent of the ground plan of an above-ground construction. The anomaly is very high in amplitude, a fact that allows the assumption that the buried features causing it were burnt. On the other hand, if these are proven to be the concealed remnants of a building, then its internal space separations are also seen in the magnetogram. Other anomalies that could indicate the presence of smaller buildings are much more faint. Some anomalies that appear as bull's eyes might have been caused by structures subjected to severe burning. Taking into account that pieces of ceramic slag were found close to the most western one, it is much likely that this particular anomaly is caused by the buried vestiges of a pottery kiln. The other anomalies of this kind might have been caused also by buried remnants of kilns, ovens or hearths.

Less strongly magnetised features appear throughout the magnetogram, both outside and inside the main ditch. Those to the east of the ditch could refer to earth roads, the others elude meaningful interpretations.

Also, many negative linear features (lighter tones) appear at the southern end of the magnetogram. They might be caused by buried remnants of structures having nonmagnetic masonry. An alternative interpretation is that they are caused by ditches which have been under stagnant water for long time intervals in combination with changes of the water table.[18] In the latter case, the partial dissolution of the ferrimagnetic particles and the

[17] Miller and Singh 1994; Stampolidis and Tsokas 2012.

[18] Fassbinder 2015.

Figure 9.2.3. Magnetogram of the prehistoric site of Elateia. Both single instrument and gradiometer array were used. The vertical gradient of the vertical component of the total magnetic field is precisely the mapped quantity. The coordinates are in the Hellenic Grid projection (Hellenic Geodetic Reference System 1987).

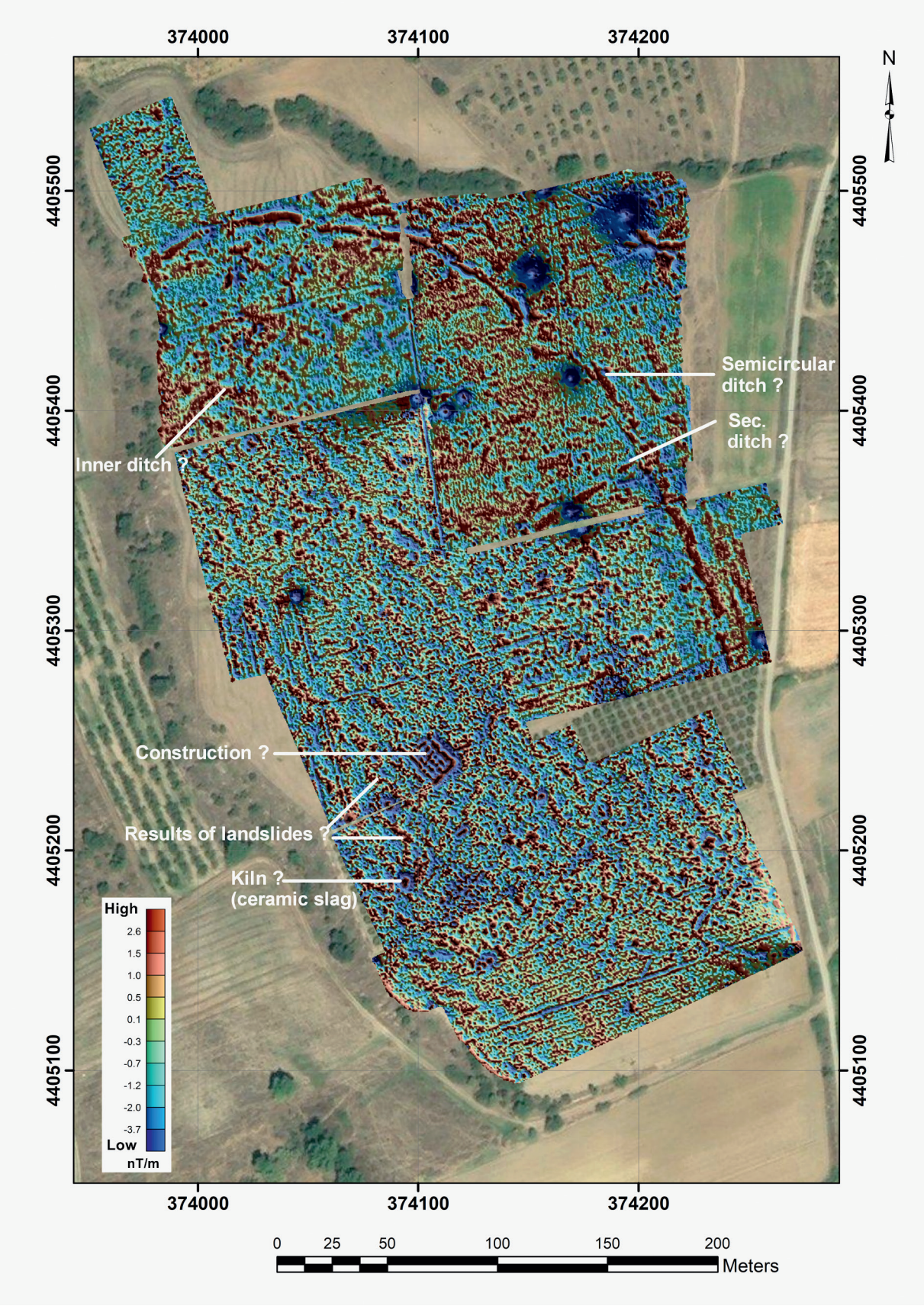

Figure 9.2.4. Tilt angle transformation of the magnetogram shown in Figure 9.2.3, with some additional interpretative notes.

precipitation of iron oxides cause the negative anomaly. A third alternative is that some small ditches were dug at the ground surface and they were immediately refilled by the same material. Thus, the magnetic particles are randomly redistributed resulting essentially in the nullification of their net magnetism.

9.2.5. The Resistivity Tomography Method

In the common electrical methods for prospecting the subsurface, two electrodes are used to conduct the current into the subsurface, whereas the created potential difference at the ground surface is measured by means of another two electrodes.[19] Next, a series of measurements is taken along profiles, using successively increased electrode spacing, aiming to record the lateral and vertical resistivity variation. These measurements (called apparent resistivity measurements) are next treated mathematically by a process called inversion, in order to yield the real underground distribution of resistivity.[20]
Inversion is a complicated mathematical algorithm that allows the reconstruction of any measured data-set independent of the electrode arrangement. Furthermore, the advent of modern recording gear provided the means for fast automation of the measuring procedure. In addition, the use of any combination of measurements (electrode arrangements) can overcome potential technical problems. The automated measuring systems together with the inversion algorithms enabled the creation of images of the distribution of the subsurface resistivity in either a two- or three-dimensional context. The whole procedure, but also the final image, is called Electrical Resistivity Tomography (ERT) because of the similar procedures of medical imaging techniques.

9.2.6. The Electrical Resistivity Tomography (ERT) and data processing

The ERT surveys carried out were exclusively aiming to examine the long, curved magnetic signature of the supposed ditch was been revealed in the north-northeast. Further, they aimed to investigate the existence of the ditch further south from the point it was last observed on the magnetogram. The layout of the profiles along which the ERTs were performed is shown in Figure 9.2.5. In fact, 14 two dimensional tomographies were carried out. Six of them, L5 to L10, were carried out so that they constitute a grid. Further, the ERT marked as L5 was remeasured as ERT_19 for checking purposes.
The dipole–dipole and the multi-gradient array were used for data collection for every ERT.[21] We followed this approach in order to gain the advantages of both arrays.[22] The inter probe spacing was set to 1.0 m for all cases. Similarly, the tomographies of the grid were also spaced 1.0 m apart from one another.
For all ERTs, 24 channels were employed and the SYSCAL-pro resistivity meter of IRIS instruments was used. The instrument allows for a maximum of ten potential measurements simultaneously. Switches, connectors and multicore cables used were custom built by the Laboratory of Exploration Geophysics of the Aristotle University of Thessaloniki.
Each individual tomography was inverted using the scheme of P. Tsourlos[23] which is based on iterative optimisation based on Finite Element modelling. The algorithm employed in this scheme was proposed by S. Constable and his team[24] and it is fully automated and self-correcting, performing smoothness constrained inversion. Thus, 2D images of the subsurface distribution of resistivities were produced.
Regarding the ERTs of the grid, they were subject also to 3D processing. In fact, it is clear that the data acquisition was not in the full 3D context. However, it has been proven[25] that data acquisition along parallel, equally spaced traverses yields a data set whose inversion by 3D algorithms is very close to what would had been resulted from a full 3D data collection.

[19] Parasnis 1997.
[20] Tsokas et al. 2009.
[21] Parasnis 1997; Dahlin and Zhou 2006.
[22] Ward 1990.
[23] Tsourlos 1995.
[24] Constable et al. 1987.
[25] Papadopoulos et al. 2006.

In the present case, data was subjected to the 3D inversion scheme proposed by P. Tsourlos and R.D. Ogilvy.[26] This is an iterative optimisation based on a 3D Finite element modelling scheme. The inversion quality control both for the 2D and 3D case was performed employing additionally the algorithms of the Korea Institute of Geology, Mining & Materials (KIGAM).[27]
The RMS error observed in all inversions was less than 3%. This is another indicator that increases the reliability of the results. In other words, we recognise that the tomographic images show a distribution of subsurface resistivities that is very close to the true distribution.

9.2.7. Results of the ERT survey

The distributions of subsurface resistivity yielded some extra clues. Figures 9.2.6–7 show the distribution of resistivity on vertical sections of the ground along the L lines of the layout in Figure 9.2.5. Generally, there is a relatively antistatic formation near the surface, which lies above a conductive substrate. Looking at the tomographies L4 to L14, they show a fairly consistent picture.
At about 2 m depth, the situation changes and many relatively high resistivity anomalies show up buried in a rather conductive environment. Considering line L11 as a guide, a distinct positive anomaly appears at the place where the ditch is expected to be about 6 m wide. The positive character can be explained assuming that coarse and dry material relative to the undisturbed environment has filled up the ditch.
The above described clear situation can be seen also at ERT_19/L5 to L14, but it is obscured by other positive anomalies from the other tomographies. These signals appear mainly eastwards of the ditch as delineated in the magnetogram. Thus, the majority of these small wave length positive anomalies appear on the outer side of the ditch. However, some small ones appear also inwards. A possible explanation for these anomalies is that they are caused by buried pits filled up again with coarser material. This means that the same causes

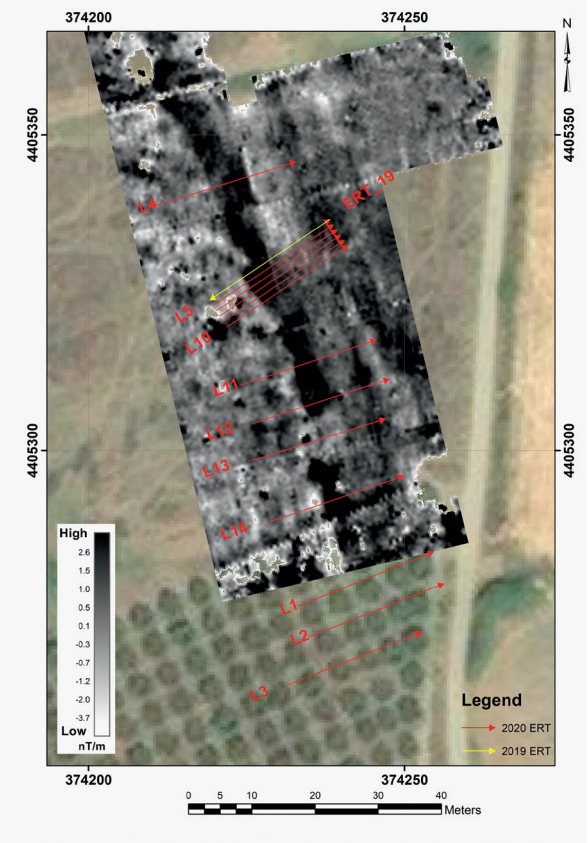

Figure 9.2.5. Layout of the ERTs carried out in the site Elateia 1 drawn on the Magnetogram. Six tomographies at the center of this figure are separated by 1 m distances such that they constitute a grid. The yellow line represents the tomography carried out for control, exactly at the position of L5, one of ERTs of the grid but with opposite direction. Also, L14 and L15 coincide; the extra tomography carried out again for control purposes.

can be considered for the electrical signature of the ditch and the pits.
The situation changes dramatically for the tomographies L1, L2 and L3. No anomaly that can be safely attributed to the ditch is present here. It seems that the electrical image represents rather the undulations of the top of some kind of substrate that has a resistive character. Alternatively, we could propose that the resistivity distribution there revealed the presence of large rocks that have been rolled down to this point. Perhaps also, that there is no ditch there.
As mentioned above, six tomographies were carried out to form a grid. Therefore, 3D processing was performed with this data and the outcome is shown in Figure 9.2.8. They suggest that the ditch may have been about 6 m wide and 2 m deep. Also,

[26] Tsourlos and Ogilvy 1999.
[27] Kim 2007.

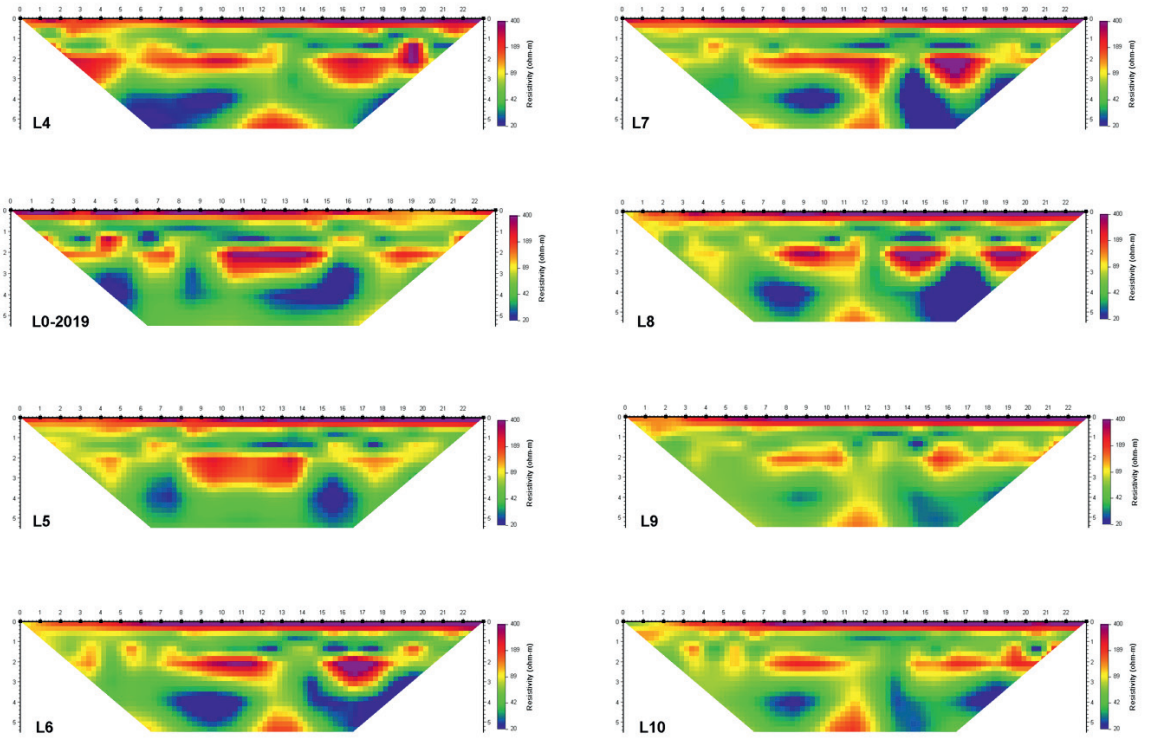

Figure 9.2.6. Tomographies L0-2019 and L4 to L10.

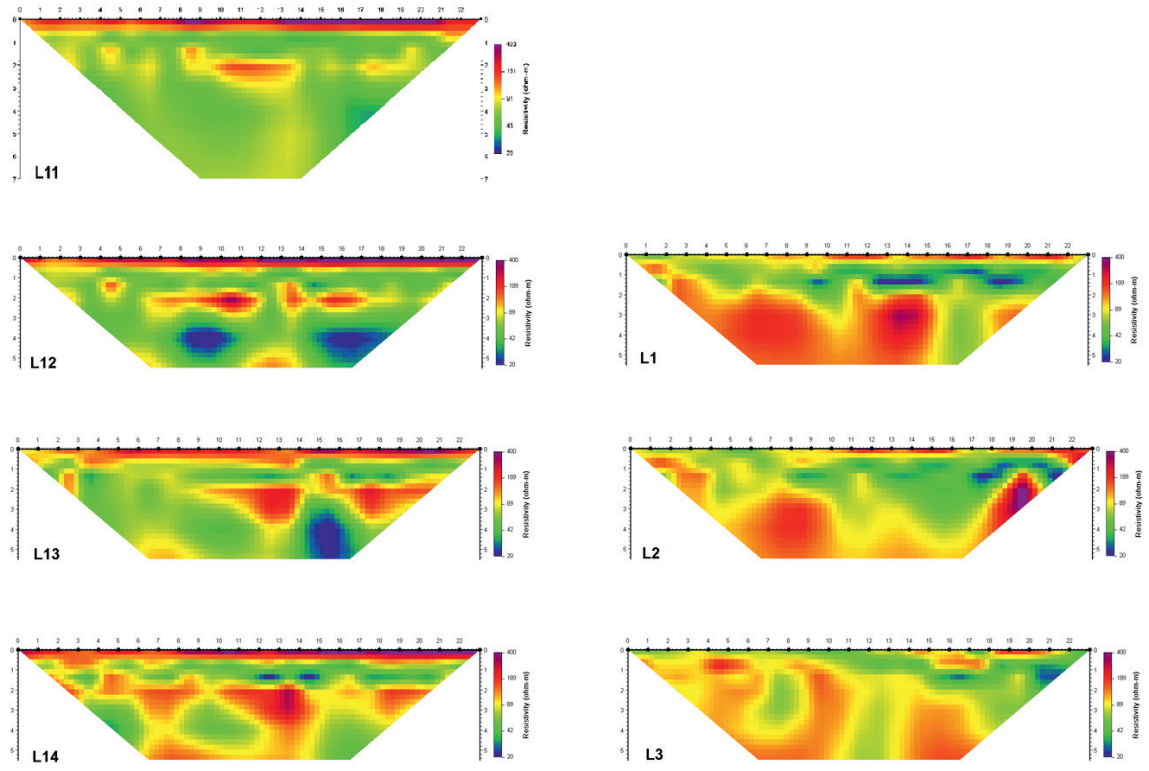

Figure 9.2.7. Tomographies L11 to L14 and L1 to L3.

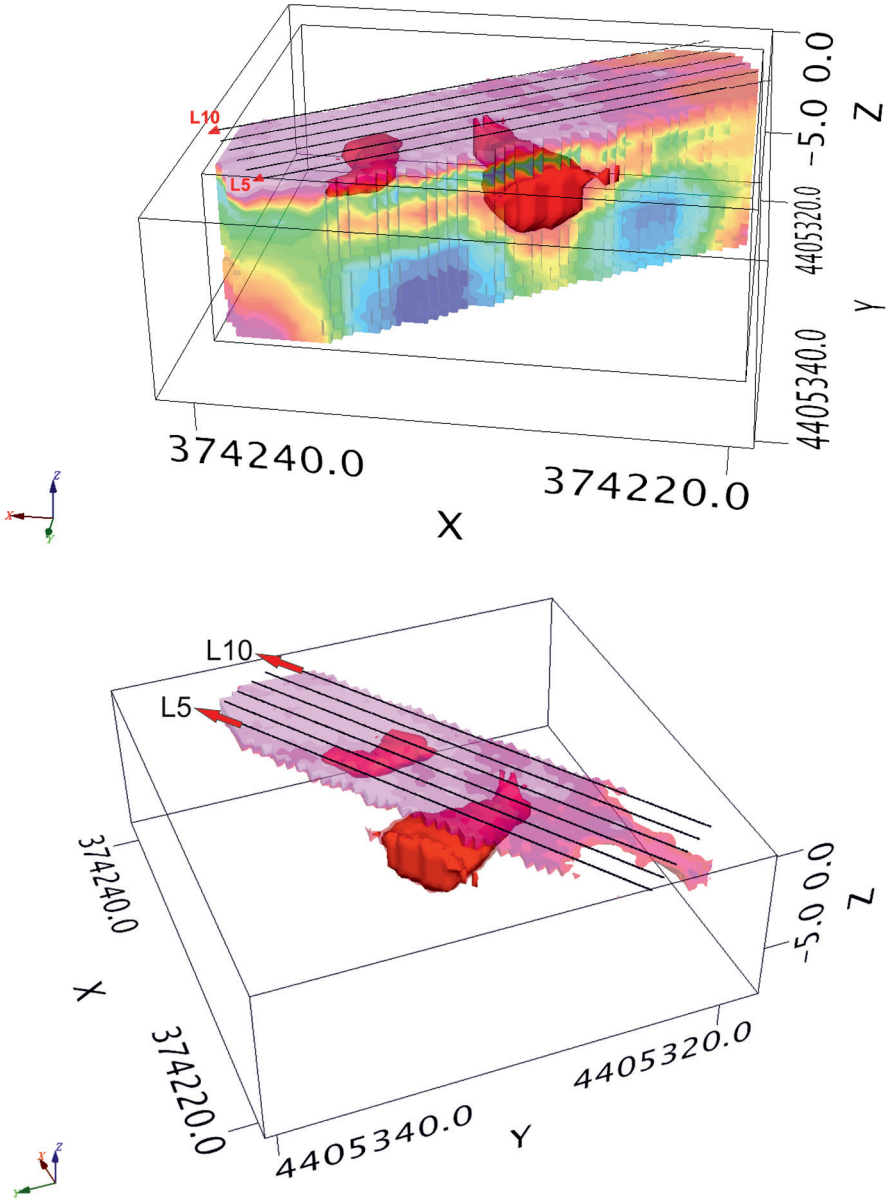

Figure 9.2.8. Three-dimensional distribution of the subsurface resistivities yielded after 3D inversion of the data of the tomographies L5 to L5. The latter had been arranged parallel so that a grid was formed.

it starts from 2 m below the present day ground surface and extends down to about 4 m depth. This result is reinforced when looking at the 3D view of the ditch.

9.2.8. Conclusions

The magnetogram of the Neolithic site of Elateia in Thessaly detected several anomalies which could be attributed to possible buried remnants of the prehistoric human occupation. The most impressive finding is the magnetic signature of a ditch, which seems to surround the prehistoric settlement from the north and the northeast. The main features of the magnetogram have been summarised in Figure 9.2.9. The tomographic examination carried out in individual sections revealed the specific resistivity of the ditch infill. This was attributed to the coarse and dry material, perhaps boulders rolled down to this point. A very good 3D image of the ditch was obtained from the grid of six tomographies which was established across the relevant magnetic anomaly. South of the last point at which the ditch appeared in the magnetogram, no signature was detected that could be assigned to the ditch.

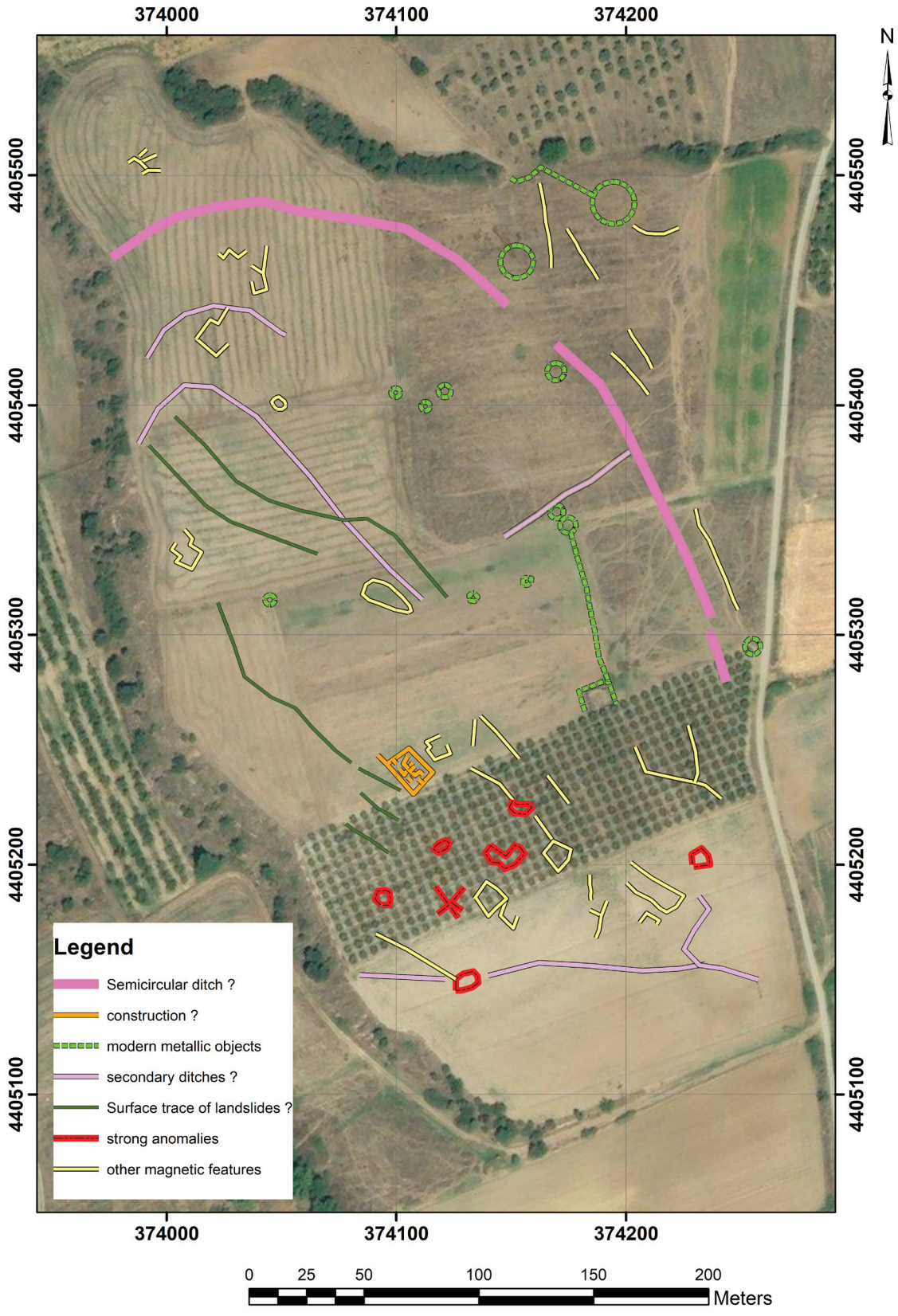

Figure 9.2.9. Interpretation map inferred from all magnetograms of the prehistoric site of Elateia.

The processed data therefore show very interesting features associated with the function of the prehistoric settlement. Not only was the presence of a ditch revealed from the curvilinear anomaly it creates on the magnetogram, but also other traces of human intervention have been detected, probably even secondary ditches.

Acknowledgements
We would like to thank the Institute of Prehistory at the Free University of Berlin who invited us to participate in the project. The funding has been assured by the German Research Foundation (DFG), Project Number 315184342.

Bibliography

Aitken 1974: M. J. Aitken, Physics and Archaeology (Oxford 1974).

Aspinall et al. 2008: A. Aspinall, C. Gaffney, and A. Schmidt, Magnetometry for archaeologists (Lanham, Maryland 2008).

Becker 1995: H. 1995, From nanotesla to picotesla – a new window for magnetic prospecting in archaeology. Archaeological Prospection 2, 1995, 217–228.

Becker 2001: H. Becker, Duo- and quadro-sensor configuration for high speed/high resolution magnetic prospecting with caesium magnetometer. In: H. Becker and J. W. E. Fassbinder (eds.), Magnetic prospecting in archaeological sites (Munich 2001) 20–25.

Constable et al. 1987: S. Constable, R. Parker, and C. Constable, Occam's inversion: A practical algorithm for generating smooth models from electromagnetic sounding data. Geophysics, 52, 1987, 289–300.

Dahlin and Zhou 2006: T. Dahlin and B. Zhou, Multiple-gradient array measurements for multichannel 2D resistivity imaging. Near Surface Geophysics 4, 2006, 113–124.

Eppelbaum 2014: L.V. Eppelbaum, Geophysical observations at archaeological sites: estimating informational content. Archaeological Prospection 21(2), 2014, 25–38.

Fassbinder 2015: J.W.E. Fassbinder, Seeing beneath the farmland, steppe and desert soil: magnetic prospecting and soil magnetism. Journal of Archaeological Science, 56, 2015, 85–95.

Fassbinder and Stanjek 1993: J.W.E. Fassbinder and H. Stanjek, Occurrence of bacterial magnetite in soils from archaeological sites. Archaeologia Polona 31, 1993, 117–128.

Fassbinder et al. 1990: J.W.E. Fassbinder, H. Stanjek, and H. Vali, Occurrence of magnetic bacteria in soil. Nature 343, 1990, 161–163.

Gaffney 2008: C. Gaffney, Detecting trends in the prediction of the buried past: a review of geophysical techniques in Archaeology. Archaeometry, 50(2), 2008, 313–336.

Karamitrou et al. 2017: A. Karamitrou, M. Petrou, and G.N. Tsokas, A pixel-based semi-stochastic algorithm for the registration of geophysical images. Archaeological Prospection 24(4), 2017, 413–424.

Kim 2007: J.H. Kim, DC_2DPRO and DC_3DPRO, User's guide. Korea Institute of Geoscience and Mineral Resources (Yuseong-gu, Daejeon 2007).

Le Borgne 1955: E. Le Borgne, Susceptibilité magnétique anormale du sol superficiel. Annales de Geophysique 11, 1955, 399–419.

Le Borgne 1960: E. Le Borgne, Influence du feu sur les proprietes magnetiques du sol et sur celles du schiste et du granite. Annales de Geophysique 16, 1960, 159–195.

Linford 2006: N. T. Linford, The application of geophysical methods to archaeological prospection, Reports on Progress in Physics 69, 2006, 2205–2257.

Linford et al. 2007: N. Linford, P. Linford, P., L. Martin, and A. Payne, Recent results from the English Heritage caesium magnetometer system in comparison with recent fluxgate gradiometers, Archaeological Prospection 14, 2007, 151–166.

Maher and Taylor 1988: B.A. Maher and R.M. Taylor, Formation of ultrafine-grained - magnetite in soils. Nature 336, 1988, 368–370.

Miller and Singh 1994: H.G. Miller and V. Singh, Potential field tilt-a new concept for location of potential field sources. Journal of Applied Geophysics 32, 1994, 213–217.

Mullins 1977: C.E. Mullins, Magnetic susceptibility of soil and its significance in soils sciences: a review. European Journal of Soil Science, 28(2), 223–246. https://doi.org/10.1111/j.1365-2389.1977.tb02232.x

Neubauer et al. 1999: W. Neubauer, A. E. Hinterleitner, and P. Melichar, Large scale geomagnetic survey of an early neolithic settlement in Lower Austria (5250–4950 BC). In: J. Faßbinder, W. Irlinger (eds.), Archaeological Prospection, Arbeitshefte des Bayerischen Landesamtes für Denkmalpflege 108, 1999, 58–59.

Papadopoulos et al. 2006: N.G. Papadopoulos, P. Tsourlos, G.N. Tsokas, and A. Sarris, 2D and 3D resistivity imaging in archaeological site investigation. Archaeological Prospection 13(3), 2006, 163–181.

Parasnis 1997: D.S. Parasnis, Principles of Applied Geophysics (London 19973).

Rassmann et al. 2016: K. Rassmann, A. Korvin-Piotrovskiy, M. Videiko, and J. Müller, The new challenge for site plans and geophysics: revealing the settlement structure of giant settlements by means of geomagnetic survey. In: Müller J, Rassmann K, Videiko M. (eds) Trypillia megasites and European prehistory 4100–3400 BCE. (New York 2016) 29–54.

Scollar et al. 1986: I. Scollar, B. Weidner, and K. Segeth, Display of archaeological magnetic data. Geophysics 51(3), 1986, 623–633.

Stampolidis and Tsokas 2012: A. Stampolidis and G.N. Tsokas, Use of edge delineating methods in interpreting magnetic archaeological prospection data. Archaeological Prospection 19, 2012, 123–140.

Tite and Mullins 1971: M.S. Tite and C.E. Mullins, Enhancement of the magnetic susceptibility of soils on Archaeological sites. Archaeometry 13(2), 1971, 209–219.

Trinks et al. 2014: I. Trinks, W. Neubauer, and A. Hinterleitner, First High-resolution GPR and Magnetic Archaeological Prospection at the Viking Age Settlement of Birka in Sweden. Archaeological Prospection 21, 2014, 185–199.

Tsokas et al. 2009: G. N. Tsokas, P. Tsourlos, and N. Papadopoulos, Electrical resistivity tomography: a flexible technique in solving problems of archaeological research. In: S. Campana and S. Piro (eds.), Seeing the Unseen. Geophysics and Landscape Archaeology (London, New York 2009).

Tsourlos 1995: P. Tsourlos, Modelling, interpretation and inversion of multielectrode resistivity survey data. PhD thesis, University of York, 1995. https://etheses.whiterose.ac.uk/14017/1/296385.pdf

Tsourlos and Ogilvy 1999: P. Tsourlos and R.D. Ogilvy, An algorithm for the 3D Inversion of Tomographic Resistivity and Induced Polarisation data: Preliminary Results. Journal of the Balkan Geophysical Society, 2(2), 1999, 30–45.

Ward 1990: S. Ward, Resistivity and Induced Polarization Methods. In: S. Ward (ed.), Geotechnical and Environmental Geophysics, vol. 1 (Investigations in Geophysics 5) (Tulsa 1990) 147–189.

9.3. Elateia 1: Interpretation of the results from the systematic archaeological and geophysical surveys

Agathe Reingruber, Giorgos Toufexis, and Amelie Mohrs

9.3.1. The flat extensive settlement Elateia 1

In spring 2018, a first geophysical survey was carried out in the central and southern area of the flat site Elateia 1. The selection of the area to be prospected was based on the results of the systematic archaeological survey and the promising Neolithic finds in this part of the settlement. In addition, five AMS dates obtained from animal bones allowed a clear assignment of the associated finds to the period 6000–5800 calBC[1], the beginning of the Middle Neolithic in Thessaly. In 2019, the study area was extended towards the north. Although in some of the fields no systematic archaeological prospections could take place due to heavy weed growth and thus poor visibility, sporadically found materials indicated an important core zone within the northwestern settlement area as well. According to the find's distribution, the whole area of ca. 10 hectares was covered by prehistoric finds, although less so in the NE. An extension of the geomagnetic investigation seemed promising and resulted in an almost integral coverage of the site (cf. Fig. 9.3.1).

The flat site of Elateia 1 lies at the foot of Mount Ossa, between two hills. It is further delimited by natural boundaries in three directions:

- towards the north by the nowadays dried out riverbed of the Tsantarli rema at 64 masl;
- the ridge towards the west, carved by the river Kalamitsa is especially steep in its central part, the difference in altitude with the level below is there of 8–10 m (74–64 masl);
- towards the south, the area ends in a rather gentle slope just before the present dirt road that may be the remnant of a paleo-riverbed;
- only towards the slopes of Mt Ossa in the east, no clear limits were identifiable, and we learned from the geophysical investigations that this part, together with the northern one, was confined by a curved linear structure. This situation corresponds to the distribution of small finds and pottery fragments: they suddenly stop west of today's dirt road (see heatmaps Figs. 9.3.6–9.3.12). We take this concurrence as clear indication for the eastern boundary of the site.

Topographically, the flat settlement lies on a slight upheaval, its highest point at approx. 78 masl (cf. Fig. 1) is in the eastern part of the site, where the large stone (Bigmeni Petra – see Chapter 10.1) is located. From here, the area slopes gently towards the northwest whereas it is more pronounced towards the southwest. The northwestern limit is slightly deeper than the southwestern one (66–68 m compared to 70–72 masl).

In the area of the upheaval, a 12-row almond grove was laid out (approx. 60 m wide and 220 m long). During or shortly after the plantation of the single trees, deeper interventions took place on the southern edge of the grove, in order to level the wheat field south of the almond grove, resulting in a steplike boundary between the fields. Not only was soil material removed but in the course of time large stones and other materials that probably disturbed the ploughing of the wheat field were deposited here. Or the stones were purposefully laid down to fix the edge of the grove – the trunks of some almond trees are already standing free due to erosion. These and other recent interventions are reflected also in the magnetogram by numerous anomalies.

The prospected fields were partly ploughed or fallow fields, and an almond grove. The two wheat fields located directly north and south of the almond grove are regularly cultivated, i.e. ploughed less than 0.50 m deep. In the almond grove, on the other hand, pits at least 0.60 m deep and just as wide must be dug for each young tree, so that deep disturbances are to be expected at regular intervals,

[1] Additionally, a very high date at ca. 6400 calBC and a very low date at 5600 calBC were obtained that are provisionally interpreted here as outliers due to insufficient collagen (compare Chapter 8.1). We cite the data with the indication 'calBC' if they have been directly obtained through radiocarbon measurements (for those dates that derive from relative chronology and by comparisons 'BC' is used).

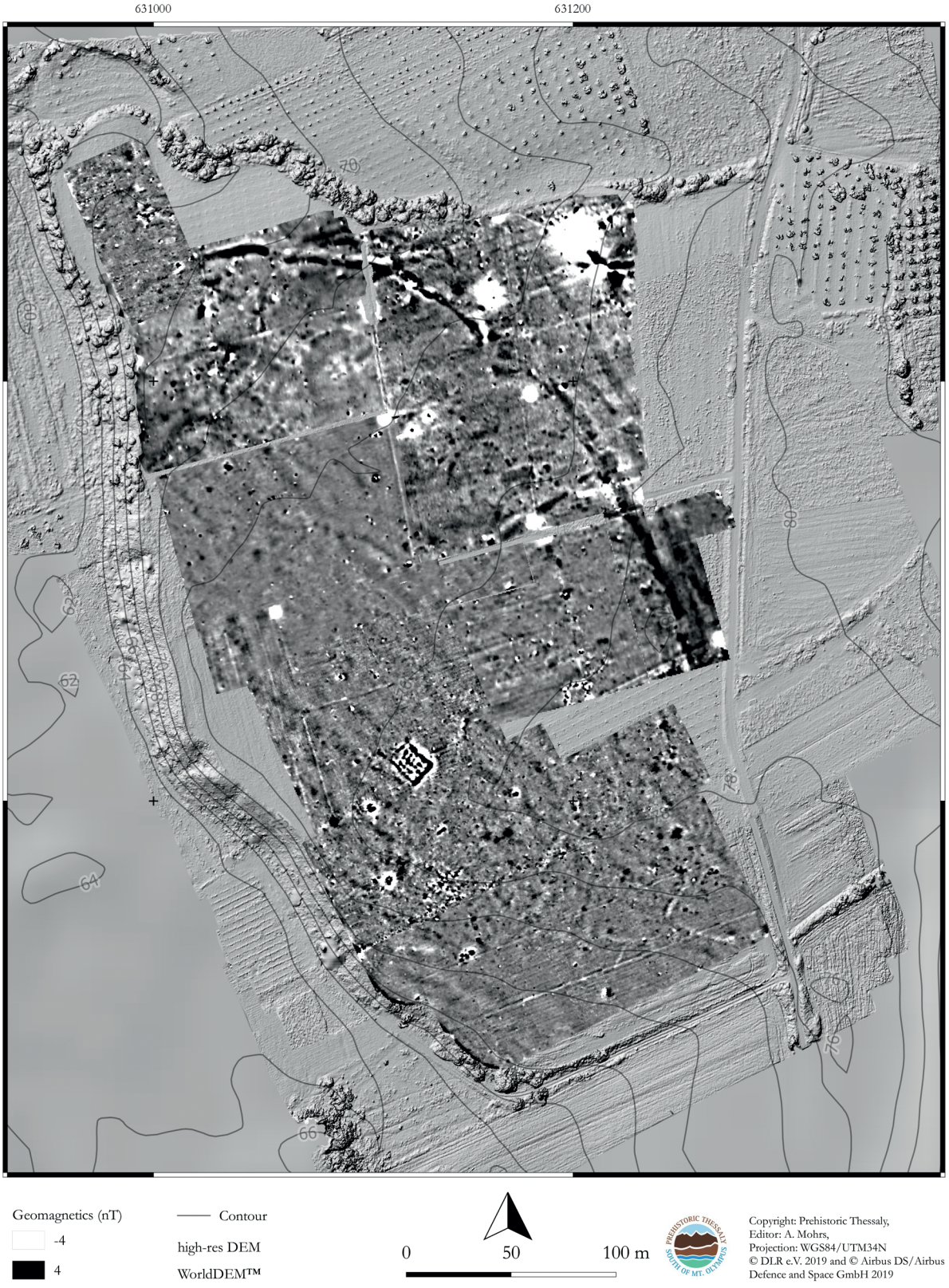

Fig. 9.3.1. The magnetogram of the settlement Elateia 1 embedded in the topographic plan. This and all subsequent grayscale images show the dynamic range from -4 to 4 nT. Thus, all higher (up to +200 nT) and lower values (up to -200 nT) are reduced to this scale to better visualize contrasts. Accordingly, they are displayed either black or white in the grayscale image with 255 values.

Fig. 9.3.2. The magnetogram, cleaned from disturbances like modern well shafts, dipoles, field boundaries and plough tracks.

as 5 x 5 m is the usual distance between the tree rows both in N–S and in E–W direction. These interventions are noticeable in the magnetogram (see below).
Apart from interventions resulted from modern agricultural activities, only few other post-Neolithic disturbances could be detected on behalf of the surface finds – therefore we suggest that most anomalies are coeval and originate from the transition from Early Neolithic (EN) to Middle Neolithic (MN), and the early MN (MN I).

9.3.2. The 'cleaning' of the magnetogram

Interfering objects in the ground generate their own magnetic fields, which stand out from the local earth's magnetic field. In the archaeological sphere, these are only minor deviations, which can have different causes. Yet extremely high nanoTesla values (henceforcth nT), over 200 nT[2], are generally regarded as (potential) modern disturbances.[3] In particular metals and reinforced concrete mixtures can be recognised in the raw data by their high values. In a first step these have been filtered out and are no longer relevant for the discussion.
One of these modern disturbances is the 100 m deep well shaft drilled directly south of the Tsantarli rema in spring 2019: the anomalies in the NE of the magnetogram (Fig. 9.3.1–2) can be based entirely on the iron and concrete construction of the well. A similar but smaller anomaly can be seen about 50 m west of this well. Interestingly, most of the anomalies considered to be modern are located in Area NE. Outstanding among them are two anomalies with a special combination of (a very small) size and (a very high) nT-value (from -110 up to 1000 nT). They too are considered to be of modern activity in this part of the prehistoric site. Other smaller and completely white signals are also due to metal inlets: Metal rods are often embedded in stone piles to mark the field boundaries.
At the northern edge of the almond grove, a sheepfold made of corrugated iron and wood has been set up, that clearly shows its signals in the magnetogram. It has been blanked out on Fig. 9.3.2, together with other black and white signals: these are dipoles formed by ferromagnetism and indicate isolated iron parts, such as fragments of e.g. agricultural equipment that was lost or left behind.
At regular intervals, deeper furrows are drawn in the direction of the plough (east-west), which are probably intended to drain rainwater. They leave linear grooves in the field. In addition, the north-south directed grooves mark field boundaries – they can also be followed up on the high-resolution DEM by Vaggelis Kremastas (compare Abb. 6.31).
All these anomalies, which can be traced back to iron use and recent activities, have been superimposed in grey in the magnetogram so that they do not further interfere with the evaluation of the archaeological anomalies (Fig. 9.3.2).
What remains for the evaluation are linear straight and curved anomalies, individual anomalies, some with a concentric black-and-white signal, and agglomerations of several small-part anomalies, for which we offer interpretations below. These must be regarded as provisional, since the nature of the anomalies can only be determined more reliably through excavations.

9.3.3. The interpretation of the anomalies suggesting potential prehistoric structures

The geomagnetically examined areas of 2018 and 2019 covered most of the settlements surface, including fields with heavy weed-growth, unploughed for many seasons, that were not prospected archaeologically. Nevertheless, we used the grid with eight areas developed from the analysis of pottery and small-finds (see Chapter 6.3, Abb. 6.39) also for the discussion of the magnetogram. Anomalies occurred in each of these areas, some of very high intensity, but the majority of low intensity, some of them clustered, others individually. Only a few of them are self-explanatory, and for this reason we have chosen to analyse each conspicuous signal by size, shape, intensity and grouping.

---

[2] Values above 200 nT have been cropped during the treatment of the data.

[3] In the literature, in some cases archaeological objects are defined as such with values up to 50 nT and those of higher values may be resulting from modern disturbances: www.ggukarlsruhe.de/GGU_Geophysik_Verfahren_Geomagnetik.html
Generally, for the assignment of the dynamic ranges, we follow Lambers et al. 2017.

Apart from the difficulties and reservations associated with their interpretations, the fact that the entire surface had been investigated both geophysically and archaeologically was indeed very helpful. In this way, the anomalies could be analysed in a broader context: linear structures could be followed up (even if apparently or repeatedly interrupted), repetitions or similarities could be identified and compared, and thus put into context.

9.3.3.1. Linear (dark) anomalies

The most conspicuous anomalies are linear alignments (Fig. 9.3.3):

- L1: a sequences of linear and slightly curved structures are confining the site towards the northeast and east ('Linear curved outer structures'). The signal is weak in the northwesternmost section, yet much stronger and accompanied by black/white contrasts with high nT-values (between -13 and 26 nT), especially in the northern reaches. After an interruption (marked by a blue arrow on Fig. 9.3.3), the signals are less but continue more clearly south of a second interruption (smaller blue arrow, at the height of L3). In this southern part, L1 is accompanied on either side by different kinds of anomalies, either linear (east of the ditch, L4b) or single roundish-irregular anomalies (to the west, inside of the ditch). It is the only case along the course of L1 with possibly associated anomalies in its inner part with values around 3–4 nT (exceptionally at -7 and 10 nT).
  L1 only seemingly ends abruptly since it continues into the almond grove but does not exit it – at least there are no indications for it farther south (compare Figs. 9.2.6–7). Therefore, L1 does not surround the whole of the settlement area. Even if erosion has been extensive near the western edge in the last millennia, it is geologically not possible that more than just a few meters only have been taken away (pers. communication by the geologist Sotiris Valkaniotis, 2018). Therefore, a symmetrical reconstruction of the ditch is impossible, even in an oval shape.
- L2: linear structures with a maximum of 2 nT are clearly visible mainly in their northwestern reaches where they produce a corner-like situation with a higher signal, up to 5 nT. Its subsequent course is less strong in the magnetogram, but it seems to continue in a southeastern direction, more or less parallel, yet more straight than the outer slightly curved structure L1.[4] Its course is also interrupted at times and seems to be accompanied by other linear and slightly curved short structures that meet with it next to interruptions (indicated by the blue arrow). Its weak signals are lost between the almond trees in the SE.
- L3: Another linear structure (at 6 nT) crosses most of the area half way up between L1 and L2. It too consists of several sections that started next to one of the interruptions in L1 and may have ended close to L2. Whether the irregular and highly magnetised anomaly L3-1 (Fig. 9.3.4) is marking the western end of L3 and is part of the structure must remain an open question.
- L4a, b: In the very east are indications for more linear structures, again up to 2 nT, that may or may not be related to L1. For the northern, slightly diagonally running L4a we have indications from historical maps that a former field path was laid out here, whose extension to the north crosses the river bed and leads to the edge of a modern plot. Towards the south, L4b merges at an acute angle with the field path used in recent times. We cannot exclude the possibility that L4b may have been part of a ditch parallel and very close to L1. Although it is not following the orbit of L1, it might have constituted a reinforcement or repair to L1 in only this specific area and may even belong to a slightly later phase, and might not have been in use simultaneously with L1.

9.3.3.2. Linear (light grey) anomalies

In the very south, the otherwise abundantly occurring signals stop abruptly: they are confined by light grey coloured lines. These linear or slightly right-angled signals (L5) are mainly located at the transition between the very 'calm', anomaly-poor

[4] Between the somewhat more prominent anomalies, more diffuse shadows appear again and again, sometimes slightly curved, but which may also be due to geology. We do not include them in our analysis for the time being.

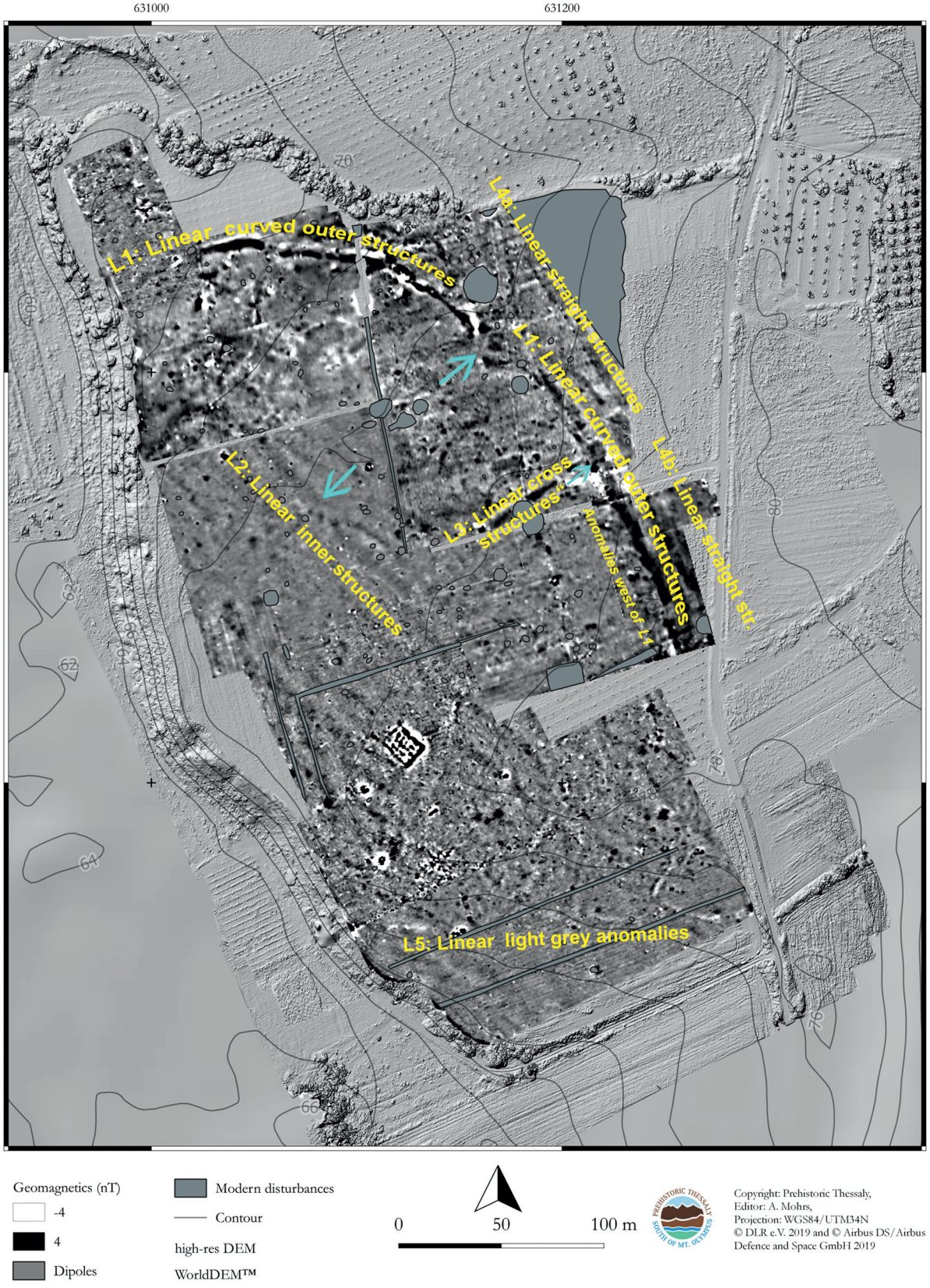

Fig. 9.3.3. Linear anomalies, possibly of the Middle Neolithic period.

Fig. 9.3.4. Interpretation of the magnetogram: Potential thermoremanent magnetisations with values above 35 nT (highlighted in red and framed with red squares) and below 35 nT (framed with orange squares); specific groups of anomalies with low signals (up to only 6 nT) are framed by light squares.

southernmost area and the much more overshadowed area directly north of it. Thus, they too are interpreted here as delimitations.
L5 with -4 to 1 nT follows the topography of the area, especially the contour lines at 74 and in the southwest at 72 masl and could be interpreted as geological signals that roughly coincide with the contour lines.[5] In another interpretation (see Chapter 9.2.4), such anomalies could indicate fringes regularly washed out by water. They may even indicate special constructions made of stones or other materials with only poor magnetic signals. In this latter interpretation they may be man-made.
A stronger but less well contoured whitish anomaly is located in the SW corner near the edge. Such whitish anomalies occur predominantly in the NW area and may be due to waters that over time have flooded and washed out this part of the settlement.

9.3.3.3. Squarish, rounded, and irregular anomalies

After the anomalies with extremely high values had been excluded from consideration (see above), in a next step we had QGIS calculate and filter out the areas with high values above 50 nT (Fig. 9.3.4). We attribute the high values to the direct influence of heat from both useful and destructive fires (kilns, hearths and ovens, fire areas and damage fires). During the cooling process the areas and/or objects were permanently magnetised, i.e. they are thermoremanent magnetised (TRM).[6] Damage fires display variable intensities, depending on the heating material involved. In the Neolithic house-context, these include wood (for posts, wattle and furniture), dry plant material (for the roofing) or grain deposits and other staple foods kept in the buildings. But also the fibres used for tempering mudbricks or daub can cause high damage to constructions since they are smoldering for many hours even after the main fire has been extinguished. The strongly magnetised areas therefore only mark those spots with extreme fire effects. Besides, burnt daub and other debris could have been discarded nearer or farther away from the focal point (dumped into a ditch[7] or into pits), thus not necessarily indicating the exact location of the event.
In addition, agglomerations of (burnt) clay fragments, broken pots, and (formerly heated) cooking stones can also change the local magnetic field and form a contrast in the magnetogram.[8]
Some very high signals occurred at the ridge in the southwest – they may (or not) be due to a miscalculation or a faulty interpolation and are not taken into account here. Also other potential interpolations will be pointed out, yet not further analysed here. The other thermoremanent magnetised structures (TRMS) will be discussed according to their position within one of the eight areas, starting from NW and ending in Area SE (compare also Table 9.3.1).
In some cases, we will additionally point out signals of less nT-values that seem of special interest. Such lower values (up to 6 nT) could be attributed to stones (as wall foundations, etc.), organic material (in pits, for example) or only little altered soil material with a slightly higher (or lower) content of iron minerals (magnetite, hematite).[9]
All the other numerous signals may all well be of prehistoric origin but for the time being they fall through our grid. To these belong, for example, series of anomalies in also roughly northwest-southeast direction, although they do not follow up exactly the orientation of L2, like those starting in between CNW-2 and -3 and ending close to CSW-1, or those leading from SW-1 towards

---

[5] This southern part of the site is a bit higher than the northern one: if water was an issue than it was rather the deeper area in the north that needed protection against rising water levels with the help of a ditch/of ditches. In the south, a simple stabilisation of the edge would suffice (e.g. by a stone alignment or a simple stone construction). In any case, the light signals in Elateia mark the southern edge of the settlement and form conspicuous angular structures. Whether they also indicate the edge of a former prehistoric lake is an assumption that would have to be verified by drillings.

[6] This term is borrowed from geology, where the results of such natural processes of heating and cooling are called thermoremanence or thermal remanence (Martin and Eiblmaier 2000–2002). While in geology the strength of remanence is measured by the unit Tesla, in archaeology the values are much lower and are given in nanoTesla. In geology, different types of magnetisations are spoken of (natural remanent or partially thermoremanent (Angenheister and Soffel 1972). Thermoremanent magnetiiation is a "Remanent magnetization acquired by a body as it cools from a high temperature" (Bucksch 1998, 506; Piro 2009, 31).

[7] Signs of TRM were identified also in some sections of the linear structure L1. They could be attributed to a secondary deposition of magnetised/burnt materials – but such an interpretation must be verified on behalf of excavations.

[8] Schenk and Goldmann 2003, 57–59; May 2018, Abb. 3–5.

[9] Patzelt and Waldhör 2019.

No.	Area and feature no.	Shape of anomaly/ies	Size of anomaly	nT (min)	nT (max)	Dynamic range	Remarks	Interpretation	No. (nT)
1	NW-1	rectangular	4 x 2.8 m	-4.5 nT	30 ntT	34.5	NW–SE orientation	structure with oven/hearth?	12
2	NW-2	roundish-irregular	4.2 x 3.6 m	-42.5 nT	107 nT	149.5	several signals overlapping	interpolation?	6
3	NE	group in curved arr.	4.9 x 2m (largest one)	1.5 nT	6 nT	4.5	semi-circle	working space? pits?	25
4	CNW-1	rectangular	18.6 x 13.6 m	-54 nT	140 nT	194	NW–SE orientation	burnt structures: kilns	4
5	CNW-2	roundish-irregular	4 x 3.8 m (9 x 6.6 m with neg. anomaly)	-61 nT	99 nT	160	primary or secondary burnt?	burnt feature: kiln?	5
6	CNW-3	roundish-rectangular	4.7 x 3.8 m	2 nT	204 nT	206	primary or secondary burnt?	debris of burnt structure?	3
7	CNW-4	group in linear arr.	10.4 x 2.7 m	-10 nT	11 nT	21	N–S orientation	living area/ working space?	15
8	CNW	group in linear arr.	4.3 x 3 m (southern one)	1.5 nT	4.5 nT	3	N–S orientation	working space/ living area?	26
9	CNE-1	roundish-irregular	5.1 x 5 m	-93 nT	135 nT	228	several signals overlapping	interpolation?	1
10	CNE-2	group	5 x 2.7 m (largest one)	2 nt	12 nt	10		living area/ working space?	22
11	CNE	group in linear arr.	3 x 3.2 m (largest anomaly in orange)	-7 nT	10 nT	17	N–S orientation	working space/ dumping area	19
12	CSW-1	disturbed	24 x 20 m	-66 nT	41 nT	107	NW–SE orientation	burnt structure (destroyed)	7
13	CSW-2	oval	4.3 x 3.3 m (7.9 x 9.3 m with neg. anomaly)	-127 nT	89 nT	216	primary or secondary burnt?	burnt feature: kiln?	2
14	CSW-3	oval	2.9 x 2.3 m (3.9 x 3.3 m with neg. anomaly)	-10 nT	70 nT	80	primary or secondary burnt?	burnt feature: kiln? oven?	10
15	CSW-4	oblong	4.9 x 1.5 m	-17 nT	54 nT	71	primary or secondary burnt?	burnt feature: kiln? oven?	11
16	CSW-5	group	6.9 x 2.4 m (southern one)	1 nT	14 nT	13	N–S orientation	living area/ working space?	21
17	CSW-6	group	4.8 x 4.6 m (largest one)	1 nT	21 nT	20	E–W orientation	living area/ working space?	16
18	CSE-1	roundish	2.8 x 2.3 m	-34 nT	73 nT	107	primary or secondary burnt?	burnt feature: kiln? oven?	8
19	CSE-2	group (disturbed?)	4.8 x 3.5 m (largest one)	-5 nT	14 nT	19	inclusive of a square anomaly	living/working area? destroyed structure?	17
20	CSE-3	group (disturbed?)	4.3 x 3.6 m (largest one)	-7 nT	14 nT	21	inclusive of a square anomaly	living/working area? destroyed structure?	14
21	SW-1	group	4 x 4.3 m (largest one)	-12 nT	73 nT	85	primary or secondary burnt?	burnt feature: kilns? ovens?	9
22	SW-2	group in linear arr.	3 x 2.4 m (largest one)	-3 nT	16 nT	19	N–S orientation	living area/ working space?	18
23	CSW-SW	group in linear arr.	3 x 1.7 m (eastern anomaly)	1.3 nT	7 nT	5.5	NW–SE	working space/ living area?	24
24	SE-1	squarish	6 x 4.8 m	-4 nT	13 nT	16		structure with oven/hearth?	20
25	SE-2	squarish	3.7 x 2.5 m	1 nT	8 nT	7		structure with oven/hearth?	23
26	L3-1	irregular	5 x 3.7 m	-5 nT	17 nT	22	several signals overlapping	interpolation?	13

Table 9.3.1. Areas and anomalies occurring within each of them.

the NW and the western edge (compare also Fig. 9.2.9: 'other magnetic features'). Nevertheless, the anomalies selected for the following analysis have provided us with a representative basis for assessing the structure and organisation of the settlement.

9.3.4. Interpretations by Areas

1. Area NW

The northern part of Area NW is rather abundant in different kinds of signals, especially directly north and south of the corner-like situation in L2 (Fig. 9.3.4). Between the linear structures L1 and L2, many small-sized anomalies appear, among them another slightly curved light-grey feature and densely grouped light grey/whitish irregular anomalies. Its southern part has not been surveyed archaeologically due to poor visibility. Yet, in the magnetogram, conspicuous anomalies appear, although few in numbers:

- NW-1: Surrounded by the northwest corner of L2, it stands out as a roughly rectangular signal with 4 x 2.8 m in size and with up to 30 nT. Its orientation is NW–SE.

- NW-2: Another anomaly (-45 to 107 nT) is slightly larger (4.2 x 3.6 m) but may be the result of the overlapping of different signals or, alternatively, an interpolation has occurred here (compare also CNE-1).

Additionally, some rather roundish single signals show low values at 0.5 to 4 nT; the biggest one is 3.5 x 4 m in size. As such, this southern area corresponds well to the findings in the northern part of CNW.

2. Area NE

In this area no TRM has been measured. Nevertheless, the magnetogram shows a plenitude of small-sized anomalies, most of them not exceeding 6 nT, comparable to those in the adjacent Area NW. They may well be of prehistoric age and, if so, rather pits than anything else.

- NE-1: Especially north of L3 appear many differently shaped anomalies, some of them as if not only grouped but even of specific (curved) alignment.

3. Area CNW

The northern part of this area is poor in anomalies. Some of low intensity appeared in the western part with dense overgrowth where no archaeological survey could be conducted: here, near the edge, a group of roundish signals in N–S-extension (in marked with a white rectangle), ca. 18.9 x 4.5 (min)/9.4 (max) m, and low nT values (0.5/1 to 5 nT) is directly neighboured in the northeast by a single irregular signal of ca. 5.9 x 3 m with low nT values between 1.5 to 3.5 nT.

Most anomalies in this area concentrate in the southern part, more or less south of the modern disturbance crossing the area in E-W direction:

- CNW-1: a rectangular and most probably above-ground structure/construction, oriented NW-SE, composed of several linear and roundish anomalies. Especially the NE and SE parts of its (presumed) foundation trench and/or of its walls show high values.[10] High signals, signs of TRM, also occur in the interior of the construction, which measures approx. 18.6 x 13.6 m (Fig. 9.3.5-a).[11] Their values up to 140 nT are evidence for either a heavy or a long or a repetitious fire that changed the clays composition.
- CNW-2: irregular anomaly, approx. 4 x 3.8 m, with a negative (white) nT value at -61 nT forming around the centre with 99 nT.[12]
- CNW-3: roundish-rectangular anomaly, approx. 4.7 x 3.8 m with only positive values up to 204 nT.
- CNW-4: A group of several anomalies seems to be part of a lengthy structure of 10.4 x 2.7 m. Their nT-values are lower than 20 (from -10 to 11 nT). Nevertheless, we define it here as a significant anomaly for reasons we will discuss below.

4. Area CNE

The area is bordered in the north by L3, and from the lateral sides by L1 und L2. Most of the anomalies are directly adjacent to L1 with values mostly at 3–4 nT (apart from a single signal at -7 to 10 nT).[13]. They seem to accompany the inner part of L1.

- CNE-1: a TRM in this area is of 5.1 x 5 m in size and directly south of a group of anomalies with less high nT-values. Like in the case of NW-2, its strong signal (-93 to 135 nT) may derive from more than two overlapping anomalies that interact with each other.
- CNE-2: a group of anomalies south of a major modern disturbance is of 12.5 x 3.5 m size and measures 2 to 12 nT.

5. Area CSW

This is the area with the highest amount of TRMS:

- CSW-1: most intriguing is the large accumulation of small anomalies with thermoremanent magnetisation (Fig. 9.3.5-b). Its maximum

[10] Comparable with e.g. the anomalies of burnt houses in the Trypillia culture (Rassmann et al. 2014a, 99–112; Rassmann et al. 2014b, 63–95). Compare also agglomeration E5 and structure E6 in Perivlepto/Kastraki 2 (Kalayici et al. 2017, Fig. 20).

[11] These and the following measures given are indicating the maximum radiations of the actual structures.

[12] This anomaly could be compared with those from Karatsandagli, e.g. structure C4 that is interpreted as the debris of clay architecture (Kalayci et al. 2017, Fig. 10).

[13] Unfortunately, this part could not be archaeologically surveyed due to the dense growth of weeds and thus insufficient visibility.

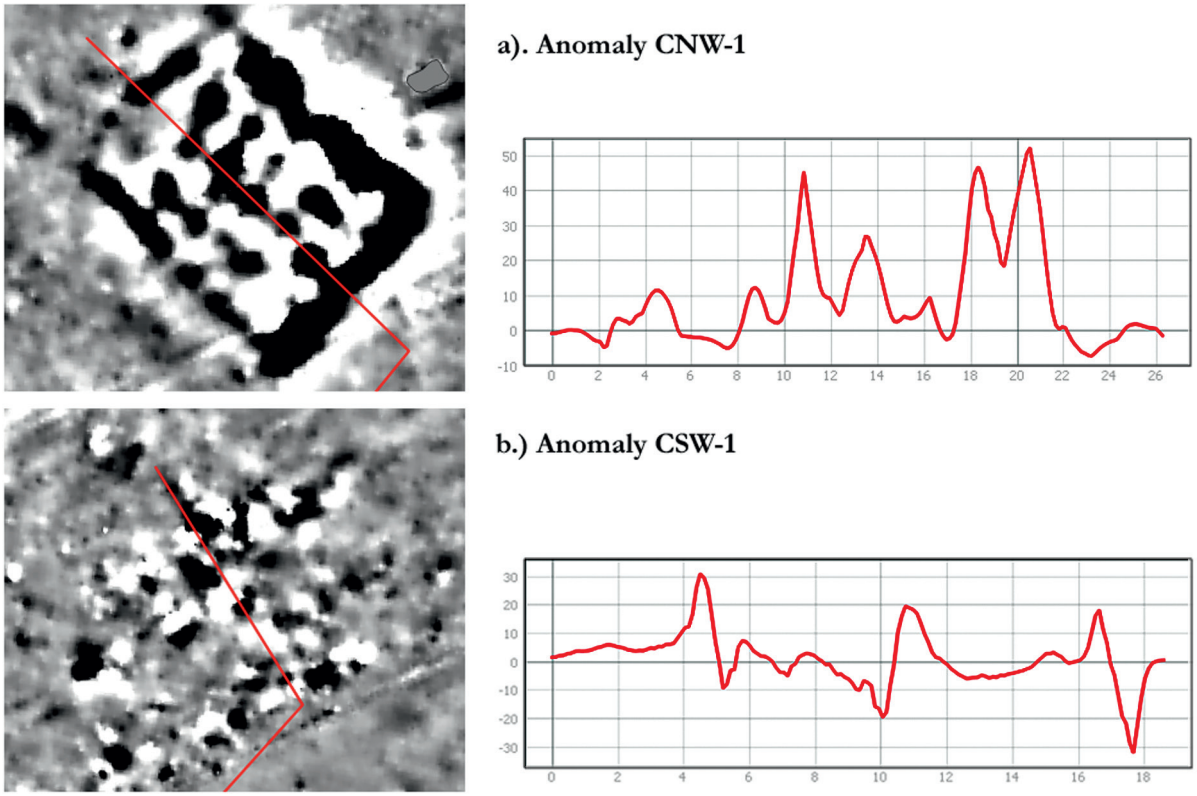

Fig. 9.3.5. Anomalies CNW-1 (a) and CSW-1 (b) next to their profiles with respective nT-values (A. Mohrs).

expansion in NW–SE-orientation is about 20 x 24 m. We interpret it, with reservations, as the remains of another large above-ground construction. It is situated in the area of the almond grove, and such trees have to be planted into pits of 60 cm depth – such interventions may have damaged the archaeological features, whereas the excavated material was certainly not taken far away, but rather littered over the nearby surface. These damages may have affected the (probably) prehistoric structure and resulted in these scattered, small-sized anomalies. A lightning strike is to be excluded due to the huge dimensions. As pointed out above, a profile edge was cut with heavy equipment directly south of these anomalies so that potentially, together with the earth, also burnt materials contained within were distributed over the adjacent surface. Note that like in the case of CNW-1, there are also roundish and oval anomalies with high dynamic ranges in the proximity of CSW-1:

- CSW-2: measures approx. 4.3 x 3.3 m without and 7.6 x 8.5 m with the negative ring around it (together at -127 nT to 89 nT).
- CSW-3: smaller oval anomaly measuring 2.9 x 2.3 m without and 3.5 x 2.6 m with the negative signal surrounding it; it too emits both negative and positive values at -10 to 70 nT.
- CSW-4: individual oblong anomaly (4.9 x 1.5 m without and ca. 6.3 x 2.9 m with negative signal) with again high nT values between -17 and 54 nT.
- CSW-5: The accumulation between CSW-1 and -2 is overshadowed by the latter and of irregular shape at ca. 7.2 x 4.8 m.
- CSW-6: East of CSW-4 three roundish anomalies appear in a roughly horizontal alignment of ca. 14 m: the easterly one is rather squarish and of 4.8 x 4.6 m, the other two are unshaped with 3 x 3 m and 3 x 5.6 m. With values between 1 to 21 nT there are no clear indications for a TRM.

6. Area CSE

Both the northern and eastern boundaries of this area were not geophysically prospected for technical reasons, which is rather unfortunate as this is where the upright stone (menhir) was found and the linear anomaly L1 would end. Compared to

Area CSW, there were only few anomalies with a clear TRM:

- CSE-1: Situated exactly at the border between areas CSW and CSE, this individual anomaly measures 2.8 x 2.3 m and has very high both positive and negative nT values from -34 to 73 nT.
  To the east lies a space with comparably few anomalies, none with TRM and of rather low nT-values, which separates it from a group of anomalies in the far east:
- CSE-2–3: This group of anomalies spreads over an area of approx. 24.5 x 11.5 m. It contains two larger, roughly square anomalies, one in CSE-2 of 4.8 x 3.5 m in size and one in CSE-3 of 4.3 x 3.6 m (the anomaly in the south-west). With only 2 to 11 nT, they do not show signs of TRM, yet these agglomerations are significant, and since they are also inside the almond grove, the damages described for CSW-1 may have similarly affected also this part of the site.

7. Area SW

Clearly at the southern limit of the site, this area, like Area SE as well, shows single or groups of anomalies only in its northern part. These must be viewed together with the adjacent northerly areas as some features straddle the borders of the areas (e.g. the group of anomalies in a white rectangle).

- SW-1: a cluster of anomalies at an almost right angle with SW-2. The four anomalies cover approx. 8.9 x 3.3 m and have a high positive (73 nT) and negative (-12 nT) magnetisation (inside the red square).
- SW-2: the north-south directed series of three roundish anomalies altogether approx. 12 m long (each signal is 2–3 x 1.6–2.4 m in size) shows a maximum of only 16 nT (inside the orange square).
  An alignment of signals leads away from this group towards the northwest, but south of SW-1 the whole area is conspicuously empty.

8. Area SE

- SE-1: A complex anomaly in the east of about 6 x 4.8 m is rather squarish in shape. The values between -4 to 13 nT do not indicate a TRM yet its size is considerable. There are some smaller anomalies west and south of it.
- SE-2 is a single, small TRM (3.7 x 2.5 m) in between many signals of different size but without strong nT-values.
  A high amount of such signals, single or in groups, are bordered towards the south by the light grey angular alignments of L5.

9.3.5. Evaluation: Four types of anomalies

According to the nT-values and the arrangement of signals, different observations can be made, both regarding the linear structure and the single or grouped anomalies. Linear structures in black (in the north) or light signals (in the south) are interpreted here as limitations, as the boundaries of the site. The northern part of the site is a few meters deeper than the southern one: if rising water levels have been an issue then protective ditches were needed especially in this area that was prone to the penetration of the flowing waters of a rivulet (the Tsantarli). L1, therefore, is interpreted here as a ditch that may have served, among other purposes, for drainage and the discharge of water.

If intrusive water was an issue in the southern part as well, then, in this area, some meters higher compared to the north, a simple stabilisation of the edge may have sufficed, e.g. through a stone alignment or a simple stone construction. And indeed, the light grey signals of L5 form conspicuous angular structures[14]. They may be man-made and may have been laid out to defend this part of the site against rising water levels. Whether they do indicate the shoreline of a former prehistoric lake is an assumption that would have to be verified by drillings.

Considering the intensity of the signals as measured by the lowest and highest nT-values of each feature under discussion (compare Tables 9.3.1 and 9.3.2), it becomes clear that some anomalies are of higher and others of lower intensity. Those of high amplitude are also the structures with a high TRM – they occur in the central-southwestern part of the site. The impact of fire – be it under or out of control – is evident (on Fig. 9.3.4 marked in

[14] Similar anomalies were interpreted by A. Sarris and his team in Karatsadagli as terrace walls or ramparts (Sarris et al. 2017, 36–39).

nT values	Dynamic range	Intensity	Remarks
from -127 to 200 nT	up to 200 nT	very high	Red on Fig. 9.3.4
from -34 to 73 nT	up to 100 nT	high	Red on Fig. 9.3.4
from -10 to 30 nT	up to 35 nT	medium high, with negative values	Orange on Fig. 9.3.4
from 1 to 30 nT	up to 20 nT	medium low, no negative values	Orange on Fig. 9.3.4
from 0.5 to 6 nT	up to 6 nT	poor, only positive values	Light shade on Fig. 9.3.4

Table 9.3.2. Anomalies grouped according to their dynamic ranges and intensities (colours correspond to those in Fig. 9.3.4).

red): Here may indeed have been the 'focal points' of dwelling activities.

Of less thermal intensity were the south-central and south-eastern areas (on Fig. 9.3.4 marked in orange). Only one such anomaly appears in the NW: here, and generally in the northern part of the site, the intensity of the signals is more reduced.

Taking further into account the intensity and size of the anomalies at least four different kinds of single or grouped signals can be recognised:

- Type 1: linear together with roundish and/or irregular signals organised in a rectangular pattern (CNW-1 and the disturbed CSW-1); they show high and low nT-values at regular distances, as visible in Fig. 9.3.5-a. The dimensions of CNW-1 are extreme for a free-standing Neolithic house, especially when considering its roofing. Therefore, rather than interpreting it as a residential building one could think of an agglutinating construction made of several smaller parts, which 'merge' into a unit in the magnetogram.[15] Another view built upon analogies with the site of Imvrou Pigadi is suggested further below.
- Type 2: single strong anomalies, roundish, oval or oblong also show a very high TRM. They may be the result of heavy fire impact on clay, either by primary fire (e.g. a kiln[16] or oven) or by secondary burning (damage fire of an above-ground structure), and, in the case of smaller anomalies, burnt debris may have been removed and redeposited (pit fills) – e.g. CNW-3, CNW-4, CSW-2, CSW-3, CSW-4; CSE-1, SW-1.

  We cannot exclude that in some cases interpolations like e.g. NW-2 or CNE-1 occurred that are probably not of archaeological relevance.

  Structure CNW-3 stands out particularly, not only because of its size with ca. 5 x 4 m but also because of its slightly rectangular shape and the lack of a white, negative ring around the black anomaly – it could very well represent the remains of a (secondary burnt) above-surface structure.
- Type 3: largely freestanding in the wider area are some anomalies of rectangular shape that, exceptionally, do display signs of a TRM with up to 30 nT. They are also noticeable due to their rectangular shape, and may have contained a hearth that shows its signals (e.g. NW-1, SE-1). By size (ca. 4 x 3 or 6 x 5 m) they are comparable with the houses from other Thessalian sites (see below). Other such rectangular signals are included in groups like CSW-5, CSW-6, CSE-2, CSE-3, SW-2. The larger ones among them also fit the sizes of MN-houses and may indicate living spaces next to working areas. Interestingly, most of them occur in the southern half of the site, but not only, and are

[15] Thus, also the large building from Almyriotiki with 10 x 25 m actually consists of three houses built close together (Sarris et al. 2017, 44). Another example, but from the LN, comes from Visviki Magoula (Sarris et al. 2015, Fig. 40b). All up to now geomagnetically detected big buildings with sizes above 10 m derive from multi-roomed structures. 1–2 roomed buildings never exceed 8–9 x 6–7 m, usually they have sizes of 4–5 x 3–4 m (Sarris et al. 2017).

[16] Compare Rassmann et al. 2014, Fig. 17 with three circular anomalies from Talianki.

interpreted here as living spaces and/or working areas.
- Type 4: most of the remaining anomalies are a) smaller in size and/or b) have values only up to 6 nT: they appear all over the site, but we point out here only those that stand out because of their special arrangement in combination with neighbouring anomalies (on Fig. 9.3.4 inside light squares). They tend to occur at the outer limits of the site and are interpreted here as indicators for working areas, adjacent to the living spaces with TMRS.

It is noticeable that strongest TRM appear in the western and southern part of the settlement and are oriented in a NW–SE direction. According to the interpretation of the magnetogram, they were confined inside an area delimited by the different linear structures forming L2 and in the area with the highest terrain level and thus secure from potentially intruding waters.

9.3.6. Interpreting the extensive flat site Elateia 1 based on the information from geophysical and archaeological surveys.

9.3.6.1. Elateia 1 in context

If we conceive of the 10 ha big area as a flat site that is composed of ditches, two large burnt structures (one of them heavily disturbed), different kinds of anomalies as described above, plus the menhir 'Bigmeni Petra' located in its highest part, then a very complex and complete settlement unfolds before our eyes for which it is difficult to find coeval comparisons. As proven by the relative chronological analysis and confirmed by radiocarbon dates, the site has been inhabited during the early MN, between 6000 and 5800 calBC.

In most EN and early MN sites, however, the above features are largely known, although not in such a verifiable context as in Elateia 1. Some of the structures and features, are better understood from later contexts of the Late and Final Neolithic (Chalcolithic), as is the case of ditches. However, we try to avoid projecting back knowledge acquired from younger sites, because in the course of 1000 or even more years, designs and functions of e.g. ditches may have changed considerably.

And ditches are among the most conspicuous features on the magnetogram from Elateia 1. They are a rather common phenomenon in Neolithic Thessaly and have been acknowledged since the very beginning of archaeological research, e.g. from Argissa and Otzaki where they were interpreted exclusively as part of defence systems.[17] Later, single or multiple ditches were also reported from many other sites belonging mainly to the Late Neolithic and Chalcolithic, e.g. Palioskala or Mandra.[18] Coeval with the ditch system from Elateia and securely dated to the transitional period EN/MN is the ditch from Makrychori 1. This magoula, located only 2.5 km west of Elateia 1, was enclosed at least from the west side, where the trenches were opened, by a ditch dug into the schist rock. It was additionally reinforced on its inner side by a mudbrick wall.[19]

Another excavation, at Larissa-Neraida, also reported a negative structure. Unlike at Makrychori 1, it was not located on the periphery of the site, but was included in the settlement area, where it may have served as an internal separation. [20]

Thanks mainly to the geophysical investigations led by A. Sarris and his team[21], we now know that ditches do indeed form an integral part of Neolithic sites. But for none of these geophysically investigated sites has an accurate relative chronological dating been presented, based on statistical analysis of pottery and finds, let alone a secure radiocarbon chronology. Besides, the sites investigated are exclusively magoules and as such only their uppermost and final occupation phase is revealed in the magnetograms, the deepest levels, be they of EN times, are not represented there.

Therefore, some of the sites might actually have been founded in the late EN or early MN, but the unity of, on the one hand, some early pottery sherds found on top of the magoules with, on the other hand, the uppermost levels has not been clarified yet. Sites supposedly labelled as EN may actually belong to the early MN or to even younger periods. And also the exact dating of the ditches has not been ascertained yet by excavation.

---

[17] Milojčić 1976; Hanschmann 1976.
[18] Toufexis 2017.
[19] Toufexis 2017, 168–171, 176–177.
[20] Anetakis 2020.
[21] Sarris et al. 2017.

Some of the ditches revealed geophysically are not continuous, but show multiple interruptions in the magnetogram, e.g. in Perivlepto/Kastraki 2[22]. In these cases, the assumption that they were designed as measures against flooding of settlements by both flowing waters or by changing levels of lakes[23] may not hold true, so that we have to think of other uses as well. Especially so, since excavated ditches are found in a variety of combinations with reinforcements both on their outer and/or their inner sides, be it palisades, earth-banks or reinforcements with wooden beams set in large postholes: such combinations have recently been systematically categorised.[24]

But not only ditches may have been used to enclose settlements: as discussed by Adrymi-Sismani, stone walls may also have been built as measures to protect a site, e.g. from water intrusion. At Thermokipia, a site from the eastern shore of Lake Karla, such walls, 0.66 to 1.50 m wide, are thought to have protected a MN building from fluctuations in the lake level.[25] It is made of single adjacent walls of different widths and with different techniques that may have been freestanding and joined into an irregular courtyard 11 x 15 m in size only in its latest phase. In geophysical measurements, stone walls appear as light shadows, as in the southern periphery of Elateia, where light linear structures may indicate stone walls.

Another very conspicuous feature in the magnetogram from Elateia is the square structure in its central part. At first sight, an interpretation as above ground, roofed construction seemed plausible. But the dimensions are huge, with ca. 19 x 14 m. Based on the excavations in Imvrou Pigadi by Nina Kyparissi-Apostolika[26], another interpretation seems more probable: that of a kiln area surrounded by thick firewalls, without a roof.[27]

In Imvrou Pigadi, several kilns were found next to each other, protected from the two excavated sides by thick and long fire-walls. These certainly would have produced strong signals in a magnetogram, very probable similar to those from Elateia 1.

Less strong signals may indeed pertain to above ground constructions and dwellings. From excavated sites is known that houses in the EN are usually ca. 4–5 x 5–6 m in size, e.g. in Argissa (EN II), Otzaki ('mittlere Schicht', EN III), Achilleion (Phase IIa)[28] and so are also the smaller houses from the MN in Sesklo and Tsangli.[29] In Koutroulou Magoula, clearly dated to the MN and coeval with Elateia 1, two buildings were unearthed, the outlines of the smaller Building 1 being completely preserved with ca. 6 x 4.5 m (28 sqm), with an opening of 2 m in its southern wall.[30] Building 2 is somewhat larger, with ca. 7.3 x 6.6 m, but its southern wall is reconstructed. They were both built with mudbricks upon a stone foundation preserved 0.3 m in height.

This kind of construction is well known from southern Thessaly and indeed, more recently such kinds of buildings were uncovered during rescue excavations in the area of Volos. In Thermokipia, a large domestic unit was revealed, consisting of a 6 x 5.50 m large house that was erected on a stone foundation preserved up to 1.22 m height, reinforced with beams.[31] This site is situated in a stone-rich region between Lake Karla and the Mavrovouni mountains, as is also the site of Omvria (Kanalia). There, a complex consisting of six rectangular rooms in two rows sharing com-

[22] Kalayci et al. 2017, Fig. 20.
[23] E.g. Sarris et al. 2017, 46
[24] Toufexis 2017, 310–312.
[25] Adrymi-Sismani 2013, 58: Alternatively, such walls may be indications of an emerging social diversification with a more differentiated organisation of space, as is known later from Palioskala and Dimini.
[26] Kyparissi-Apostolika 2012, Fig. 8–11. We would like to thank Director em. Dr. Nina Kyparissi-Apostolika for inviting us to visit the site and share her thoughts with us.
[27] In Chalki 1, G. Toufexis excavated in 1994 part of a pottery kiln with fire holes, also dating to the early MN.
[28] Milojčić 1962, Plan V; Milojčić 1971, Plan VIII; Gimbutas et al. 1989, Abb. 4.3–4.4.
[29] Theocharis 1973, Fig. 177–179: The famous 'potters shop' in Sesklo is with 7 x 5,5 m a bit larger (Theocharis 1973, Fig. 183–184), whereas the 'House P' in MN-Tsangli is ca. 7,8 x 8,5 m (Theocharis 1973, Fig. 188–189). In the EN of Thessaly, only few house floor plans were up to now documented, mostly incomplete (e.g. Wijnen 1992), and, unlike Macedonia with e.g. Mavropigi or Nea Nikomedeia, no precise settlement plan exists (Pyke 1996). The magnetograms published as EN by Sarris et al. 2017 or Kalayci et al. 2017 have not been conclusively dated neither by relative nor by absolute chronology.
[30] Kyparissi-Apostolika and Hamilakis 2015; Papadopoulos et al. 2015, 1036 and Fig. 1.
[31] Adrymi-Sismani 2013a, 51–58, 2013b, 2014. It has been dated by the excavator to the later MN but there are indications for a preceding, older building. To it belonged the stone enclosure described above.

mon mud brick walls on stone foundations was found during rescue excavations in 2007.[32]
This short overview shows that houses in the early MN, usually 5 x 4 m in size, were built of wattle and daub, pisé, mudbricks, with or without wall foundations – materials which, when burnt, show a high thermo-magnetisation and leave a clear indication in the magnetogram.
Pits are a recurring element of each Neolithic site and can be of different usage. In Argissa Magoula, a pit of oval shape (2,60 x 2 m) had been dug 1 m deep into the virgin soil ('Grube α'). It showed straight walls and was lined with a 10–12 cm thick layer of clay, the reason why it was interpreted by the excavator as a grain silo.[33] Alternatively, it may have been used for cooking, especially since mainly animal bones and 151 broken pebbles that showed signs of cracks from heating were found together with 58 completely preserved pebbles.[34]
Fire pits have been observed also in Achilleion: There, a fire pit from phase IIa was lined with a layer of pebbles and it contained ash mixed with stones and bones; near its rim, on one side only, was a horseshoe-shaped clay wall preserved. Another example from Achilleion phase IIIb contains stones of various sizes.[35] From the Thessalian Neolithic, no such features have yet been geophysically prospected and additionally excavated, so their existence needs still to be proven, but those from Achilleion do resemble the examples of pits containing cooking stones from Seddin, Brandenburg.[36]
Some of the pits in Elateia 1 form linear or slightly curved groups of pits. They are particularly conspicuous north of L3, in the intermediate area between the two linear structures. Judging by their small, dark signals, the use of heated material inside them can be suggested.

[32] Almatzi 2012, 127–136.
[33] Milojčić 1962, 12 and Plan IV.
[34] Reingruber 2008, 136.
[35] Winn and Shimabuku 1989, Fig. 4.9; 4.30.
[36] Compare May 2018: A linear arrangement of small anomalies in Seddin could be demonstrated by excavations as series of pits containing cooking stones. This finding is not mentioned here because of its ritual expressiveness, but to show what could be hidden behind such exclusively black, round, small-sized signals. It has been proven at many sites in Europe that stones were used for cooking even later in the Neolithic.

9.3.6.2. The extensive flat site Elateia 1: a complete (and unparalleled) settlement structure

The geomagnetic investigations of 2018–2019 created a complex and all-encompassing picture of the settlement that is especially useful when overlain by results obtained from the statistical analysis of the finds. The settlement is structured by the linear anomalies L1 and L2, more or less parallel, connected by a third alignment of anomalies (L3). They differ thus considerably due to their shape and their nT-values and may have served different purposes. Outside the outer linear structures, only few disturbances in the earth's magnetic field can be detected, mostly dipoles and modern interventions. This area may be described as off-site. Thus, the maximum extent of the flat Neolithic settlement has been determined geomagnetically.
This finding is confirmed by the distribution pattern obtained from archaeological surface finds (see heatmaps) and this agreement achieved with two such different methods supports and substantiates our interpretations.
The 'Linear curved outer structure' (L1) is interpreted here as a ditch. It is regularly curved and ends in the almond grove. In its northern part it shows signs of TRM (below 35 nT) possibly resulting from in-fills of burnt materials. In its southern part it is accompanied on either side by different kinds of anomalies, be them linear (L4b, an old field-path?) or single roundish-irregular anomalies (remains of negative or positive features inside of the ditch). The course of L1 consists of individual segments interrupted by oval-rectangular structures. These can be interpreted as accesses to the site. From such an access, the one in the east, the 'Linear cross structure' (L3), interrupted at least in three positions, leads to the 'Linear inner structure' (L2). L3 is perpendicular to both L1 and L2 and thus seems to have connected them. It may derive from a structure that separated this intermediate area into a northwestern and a southeastern zone.
The 'Linear inner structure' (L2) surrounds the westernmost part of the settlement and may have served as a boundary or delimitation. It is of slightly angular appearance in its northeastern ending and is accompanied here by many small roundish anomalies. In its further course it also seems to be

made of several fragments with interruptions[37] that correspond to interruptions of the 'Outer Ditch' (L1). Slightly curved (potential) anomalies lead to at least one of the openings of the 'Inner Ditch' – with three larger anomalies in their midst (left blue arrow on Fig. 9.3.3).

What is noticeable in the intermediate area between the two linear structures, especially north of L3, are the numerous small, dark signals that seem to be arranged in groups. Some of them form linear or slightly curved accumulations. No rectangular structures are detectable here that could be interpreted as buildings. Rather, the measurements indicate a magnetically less conspicuous area with only few TRM-anomalies, and as such more homogenous as the rest of the site. Therefore, we interpret this part as an open space within the boundaries of the settlement, with less intensive above ground building activities but with many anthropogenic interventions into the soil. These areas may have been used for special economic purposes (e.g. food preparation, slaughtering of animals, gardening).[38] Yet, a certain restlessness is caused by groups of light greyish to white signals that affect mainly the northern area (see below): they could indicate that the area was repeatedly covered and washed out by penetrating water.

Also the heatmap of the decorated sherds shows a conspicuous emptiness in this part (Fig. 9.3.6). Only a few such sherds were found directly south of L1, both north and south of L3. A completely different picture emerges in the western part of the site, west of L2, where four hotspots of decorated sherds appear:

- one in Area NW, close to anomaly NW-1;
- one above the rectangular structure CNW-1;
- one overlaying the alignment east of it (CNW-2).
- one appears directly southeast of CSW-1 and may be related to it.

Hotspots of less intensity spread over the southern areas, in and south of the almond grove. They confirm in some cases the observations made on behalf of the magnetogram: In the western part of areas CSE/SE, only few decorated sherds appeared and this is the case also for anomalies of high intensity. But in the very east of these two areas many more decorated sherds were collected, resulting in concentrations that can be connected to the groups of anomalies in CSE-3, SE-1 and SE-2. Last but not least, SW-1 can also be connected to a hotspot in the heatmap.

Other hotspots, less pronounced, develop in between the mentioned ones, indicating more social activity in the parts they cover. They hardly directly overlay the type2-signals, but occur next to them. If type2-signals were to be interpreted as the debris of heavily burnt above-ground dwellings and no decorated pots have been used within them, then this discordance may be due to dislocations of sherds during the millennia or the discarding of possibly broken pots next to (or farther away?) from houses. However, it is more plausible that the TRM did not originate from a secondary fire, but from the targeted work with heat in above-ground ovens or underground pits, where food or clay or any other material was transformed with the help of heat or of open fire. These presumably were not residential, but rather working areas.

Another proxy for the usage of the settlements' space are small finds like figurines, beads or items of daily usage like spoons made of shell (Fig. 9.3.7): They too concentrate in the west and south, more or less overlaying the hotspots with special sherds in features NW-1, CNW-2, SW-2 and SE-1. Not surprisingly, the marble vessels do match well with these special objects, reinforcing the hotspots above CNW-2, SW-1 and SE-1 and CSE-2. Therefore, we assume that not necessarily the areas with a very high TRM (above 50 nT) were initially living spaces but more often those below 30 nT.

When contrasting these findings with the ground stone tools they show very different agglomerations or hotspots (Fig. 9.3.8). This is especially the case with Area CNE and the northern part of CNW, where the proposed working areas were located: west of L2 occurred mainly pestles and east of L2 mainly grinding slabs and pounders made of quartz. Indeed, some of the other stone tools appear within or close to the hotspots of the decorated sherds but many of them do not, as is the case of cutting tools made of serpentinite. They were often located in 'empty spaces' like the one in the far south or in between Areas SW and SE and even in Area CNE,

[37] Interruptions are known also from other sites, e.g. Perivlepto/Kastraki 2 (Kalayci et al. 2017, Fig. 20).

[38] Magnetically empty areas were also detected at other Neolithic settlements, e.g. in Karatsantagli or in Perivlepto/Kastraki 2 (Sarris et al. 2017; Kalayci et al. 2017).

Fig. 9.3.6. Heatmap based on decorated sherds.

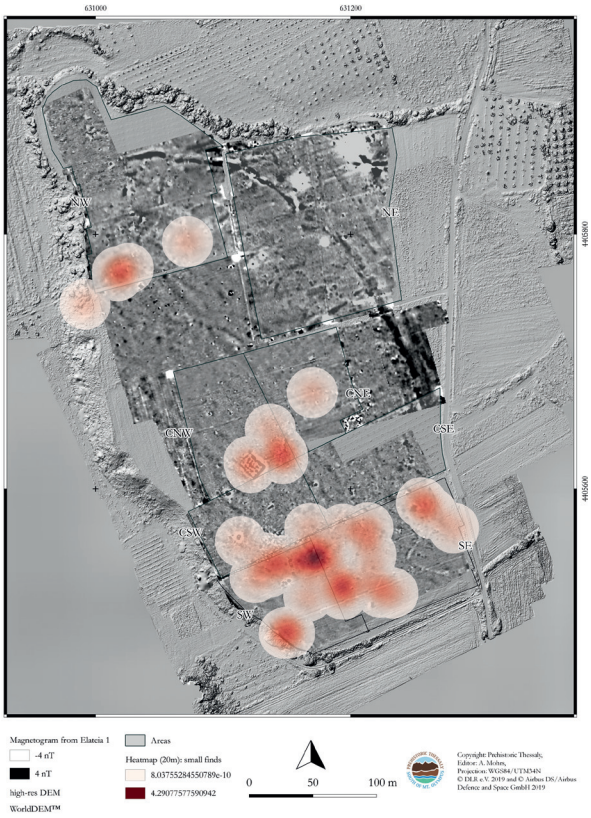

Fig. 9.3.7. Heatmap based on small finds (clay and shell).

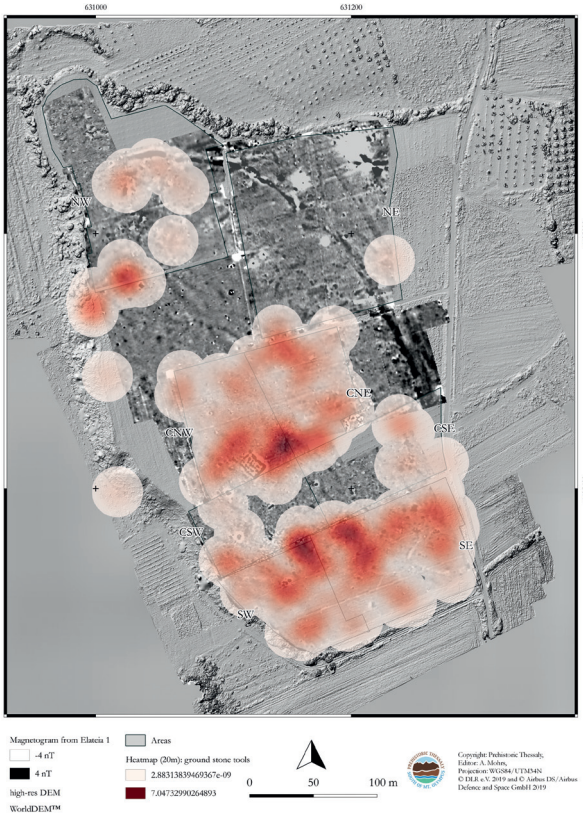

Fig. 9.3.8. Heatmap based on ground stone tools.

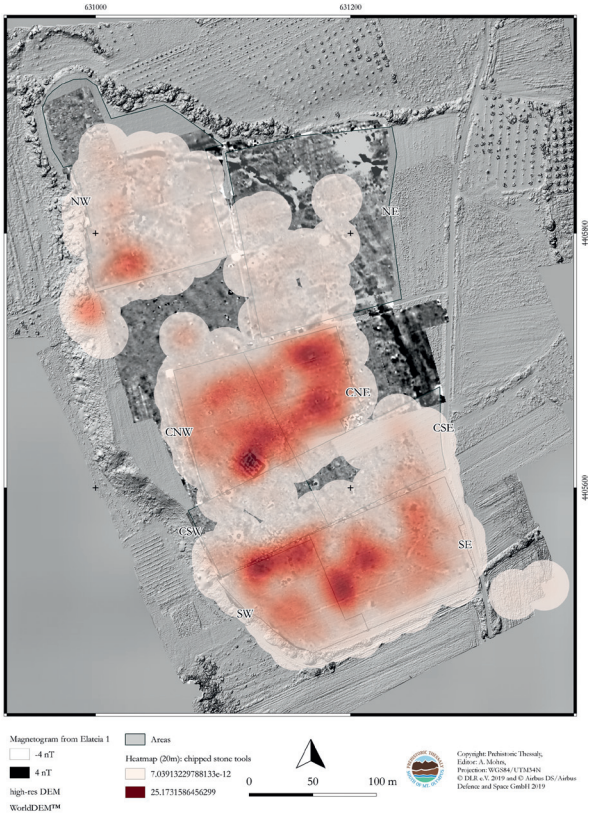

Fig. 9.3.9. Heatmap based on chipped stone tools.

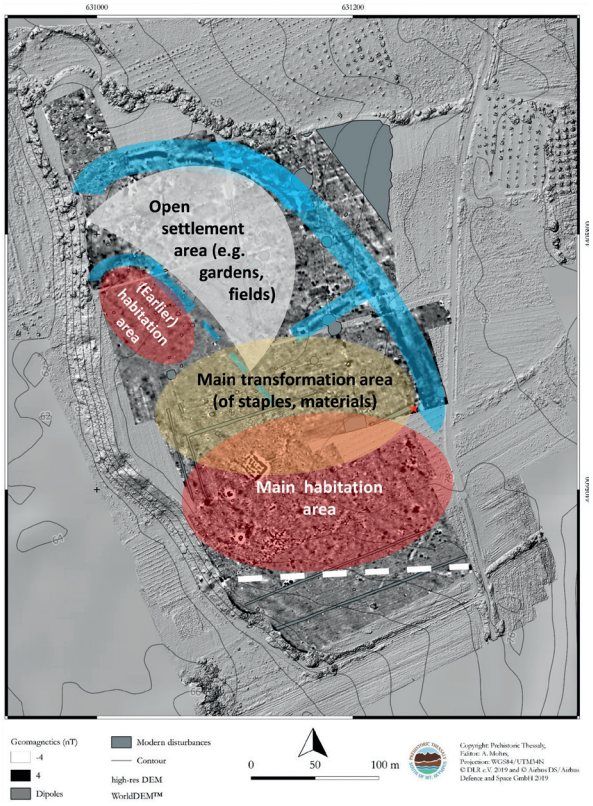

Fig. 9.3.10. Interpretation plan of the flat extended settlement Elateia 1 confined and separated by ditches (accentuated in blue hue) and dry masonry (white dashed line), with an earlier and a later (mainly) habitation area, a central part for (mainly) food processing and a northern part for gardening. The location of the 'menhir' close to the ditch is indicated by a red star.

otherwise poor in finds, and here especially directly south of L3. Here, a small observation may by allowed: Animal bones were collected again mainly in the areas with decorated pottery but often outside or in between such areas, e.g. in CNE, directly south of L3. Bones and cutting tools together could indicate areas of slaughtering or food preparation and consumption.

A good match with the ground stones is shown by the chipped stone tools (Fig. 9.3.9), except for one important difference: This is the only category we found close to the northern part of the ditch. This may support the view according to which gardens were located here with crops that were harvested with chipped stone tools. And it leads us to the conclusion that the course of L3 has structured the layout of the settlement in this area decisively, separating it into a northeastern part with plenty of pits, even tightly clustered ones, some with a specific alignment (curved), but without any special finds except for lithics. To the contrary, the southeastern part is abundant in grinding stones and some animal bones.

As generally known, water was, and still is, of utmost importance for the choice of a settlements' location. Water seems to have been a main issue not only in the selection of this spot for settling down at the end of the EN but also for its abandonment during the MN. We suggest that during the two centuries of occupation, the water levels have risen constantly, requiring at an early stage in the site's occupation the digging of a drainage ditch for protecting and controlling the 'open spaces' adjacent to L1. Whereas the core of the settlement seems to have first been in the NW, at a certain stage a shift towards the presumably drier southern area took place (compare Chapter 6.3.1.7.4.), but eventually the abandonment of the whole area was inevitable. The fact that the site has not been settled again over the millennia is not really explicable, but exactly this is an extraordinary stroke of luck for the systematic investigation of this large flat area.

The anomalies in the magnetogram together with hotspots of different find categories as calculated statistically in the heatmaps can thus be considered as reliable sources for the general interpretation of the site. Although all of the finds were collected from the surface they are an important source of information, especially when put into context.

Even more: Elateia 1 is until now the only extended flat site in Eastern Thessaly that has been almost completely covered both by geophysical investigations and by systematic archaeological survey. Both the geophysical and the archaeological surveys indicate that the core area of the settlement may have been in the western part, inside the ditch L2 and in the southern area (north of structure L5). Relative and absolute chronology place the site into the first two centuries of the MN: therefore, unlike many other geophysical investigations, we are able to reliably date the features appearing in the magnetogram. Moreover, we have developed a model of how the space may have been used by its inhabitants, with living and working areas, spaces for cultivation and for food processing and a horizontal shift in locations (Fig. 9.3.10; compare

also Fig. 6.43). Such shifts may have occurred also at other sites, e.g. at Visviki Magoula[39] or even in Sesklo[40].

Finally, we were able to disclose one of the major problems people were confronted with before eventually leaving the site: a possible rise of the water table and inundations impaired at least the northern areas with open spaces for cultivation, but maybe also other parts of the settlement (compare Fig. 6.36). Climate and environmental changes have always been a big challenge for mankind.

It has become evident that based on the synthesis of two non-destructive methods, the archaeological and the geophysical survey, reliable and new information can be obtained that serves as a basis for both archaeologists and for the cultural heritage management[41] and the protection of archaeological sites. Certainly, only excavations can confirm (or refute) the model we presented here.

[39] Sarris et al. 2015, 573–578. There, a shift from the NE, the area closest to the Lake Karla, towards the SW is observable, where the place was then constantly inhabited, resulting in the magoula of the LN.

[40] Reingruber 2024, 95.

[41] Compare also Cozzolino et al. 2018.

Bibliography

Adrymi-Sismani 2013: V. Adrimi-Sismani, Agrotes kai Psarades: Para Kallinaon Boibian Limnan. Anaskamma 6, 2013, 49–62.

Almatzi 2012: K. Almatzi, Evrimata Neolithikis periodou, BA tis Magoulas 'Visviki' sta plaisia tou ergou 'Agogos Apagogis Omvrion Ydaton' tis VIPETBA. In: A. Mazarakis-Ainian (ed.), Archaeologiko Ergo Thessalias kai Stereas Elladas 3, Praktika Epistimonikis Synantisis, Volos 2009, Tomos I: Thessalia (Volos 2012) 127-136. [Greek title: K. Αλματζή, Ευρήματα Νεολιθικής περιόδου, ΒΑ της Μαγούλας «Βισβίκη» στα πλαίσια του έργου «Αγωγός Απαγωγής Ομβρίων Υδάτων» της ΒΙΠΕΤΒΑ, ΑΕΘΣΕ 3 (2009), Τόμος Ι:Θεσσαλία (Βόλο 2012) 127–136].

Angenheister and Soffel 1972: G. Angenheister and H. Soffel, Gesteinsmagnetismus und Paläomagnetismus. Studienhefte zur Physik des Erdkörpers (Berlin, Stuttgart 1972).

Anetakis 2020: M. Anetakis, Synoikia Neraida, Odos Ikarias 80 (oikopedo Papageorgiou). Archaeologiko Deltio 69, Chronika B 2014 (2020), 1434–1436.

Bucksch 1998: H. Bucksch, Wörterbuch GeoTechnik; Dictionary Geotechnical Engineering: Band II.2, Springer Verlag (Berlin, Heidelberg, New York 1998).

Cozzolino et al. 2018: M. Cozzolino, E. Di Giovanni, P. Mauriello, S. Piro, D. Zamuner, Geophysical Methods for Cultural Heritage Management (Springer Geophysics 2018).

Gimbutas et al. 1989: M. Gimbutas, S. Winn and D. Shimabuku, Achilleion: A Neolithic Settlement in Thessaly, Greece, 6400–5600 BC. Monumenta Archaeologica 14 (Los Angeles 1989).

Hanschmann 1976: E. Hanschmann, Die Funde der frühen und beginnenden mittleren Bronzezeit auf der Argissa-Magula. In: E. Hanschmann und V. Milojčić (ed.), Die deutschen Ausgrabungen auf der Argissa-Magula in Thessalien III. Die frühe und beginnende mittlere Bronzezeit. Beiträge zur ur- und frühgeschichtlichen Archäologie des Mittelmeer-Kulturraumes 14 (Bonn 1976) 21–235.

Kalayci et al. 2017: T. Kalayci, F.-X. Simon, and A. Sarris, A Manifold Approach for the Investigation of Early and Middle Neolithic Settlements in Thessaly, Greece. Geosciences 2017, 7, 79. doi:10.3390/geosciences7030079

Kyparissi-Apostolika 2012: N. Kyparissi-Apostolika, Indications of the presence of Middle Neolithic pottery kilns at Magoula Imvrou Pigadi, SW Thessaly, Greece. Documenta Praehistorica 39, 2012, 433–442.

Kyparissi-Apostolika and Hamilakis 2015: N. Kyparissi-Apostolika and G. Hamilakis, Archaeologiki kai Ethnographiki erevna sti thesi Koutroulou Magoula Phtiotidas 2009-2012. In: A. Mazarakis-Ainian (ed.), Archaeologiko Ergo Thessalias kai Stereas Elladas 4, Praktika Epistimonikis Synantisis, Volos 2012, Tomos II: Sterea Ellada (Volos 2015) 969–978. [Greek title: Αρχαιολογική και Εθνογραφική έρευνα στη θέση Κουτρουλού Μαγούλα Φθιώτιδας 2009–2012, ΑΕΘΣΕ 4]

Lambers et al. 2017: L. Lambers, J.W.E. Fassbinder, St. Ritter, and S. Ben Taher, Meninx – Geophysical prospection of a Roman town in Jerba, Tunisia. In: B. Jennings, C. Gaffney, T. Sparrow and S. Gaffney, 12th International Conference of Archaeological Prospection (Oxford 2017), 135–137.

Martin and Eiblmaier 2000–2002: C. Martin and M. Eiblmaier (eds.): Lexikon der Geowissenschaften in sechs Bänden. Spektrum, Akad. Verlag (Heidelberg 2000–2002).

May 2018: J. May, Fokussieren, Positionieren, Schritthalten: Aspekte von Raum und Zeit am „Königsgrab" von Seddin in der Prignitz. In: M. Aufleger and P. Tutlies (eds.), Das Ganze ist mehr als die Summe seiner Teile. Festschrift für Jürgen Kunow anlässlich seines Eintritts in den Ruhestand. Materialien zur Bodendenkmalpflege im Rheinland 27. LVR-Amt für Bodendenkmalpflege im Rheinland (Bonn 2018) 405–418.

Milojčić 1962: V. Milojčić, Die präkeramische neolithische Siedlung von Argissa in Thessalien. In: V. Milojčić (ed.), Die deutschen Ausgrabungen auf der Argissa-Magula in Thessalien I. Beiträge zur ur- und frühgeschichtlichen Archäologie des Mittelmeer-Kulturraumes 2 (Bonn 1962) 1–25.

Milojčić 1971: V. Milojčić, Die deutschen Ausgrabungen auf der Otzaki-Magula in Thessalien I. Das frühe Neolithikum. In: V. Milojčić (ed.), Beiträge zur ur- und frühgeschichtlichen Archäologie des Mittelmeer-Kulturraumes 10 (Bonn 1971) 5–17.

Milojčić 1976: V. Milojčić, Die Stratigraphie der frühen und beginnenden mittleren Bronzezeit auf der Argissa-Magula. Die Baubefunde. In: E. Hanschmann, V. Milojčić (ed.), Die deutschen Ausgrabungen auf der Argissa-Magula in Thessalien III. Die frühe und beginnende mittlere Bronzezeit. Beiträge zur ur- und frühgeschichtlichen Archäologie des Mittelmeer-Kulturraumes 14 (Bonn 1976) 7–19.

Milojčić 1983: V. Milojčić, Otzaki-Magula II. Die mittelneolithische Siedlung. In: V. Milojčić (ed.), Die deutschen Ausgrabungen auf der Otzaki-Magula in Thessalien II. Beiträge zur ur- und frühgeschichtlichen Archäologie des Mittelmeer-Kulturraumes 20 (Bonn 1983).

Papadopoulos et al. 2015 : C. Papadopoulos, Y. Hamilakis, and N. Kyparissi-Apostolika, Light in a Neolithic dwelling: Building 1 at Koutroulou Magoula (Greece). Antiquity 89(347), 2015, 1034-1050 (DOI: 10.15184/aqy.2015.53).

Patzelt and Waldhör 2019: A. E. Patzelt and M. Waldhör, Methode - Geomagnetische Prospektion in der Archäologie Das Prinzip der magnetischen Ortung. Terrana Geophysik. http://www.terrana-geophysik.de/images/Methode_Geomagnetik.htm (27.08.19)

Piro 2009: S. Piro, Introduction to geophysics for archaeology. In: S. Campana and S. Piro (eds.), Seeing the Unseen. Geophysics and Landscape Archaeology (London, New York 2012) 27–64.

Pyke 1996: G. Pyke, Stratigraphy. Structures and Architecture. In: K.A. Wardle (ed.), Nea Nikomedeia I: The Excavation of

an Early Neolithic Village in Northern Greece 1961–1964. The British School of Archaeology at Athens, Suppl. Vol. 25 (London 1996) 9–53.

Rassmann et al. 2014a: K. Rassmann, M. Videjko, D. Peters, and R. Gauss, Großflächige geomagnetische Untersuchungen einer kupferzeitlichen Siedlung der Trypillia-Kultur. Aktuelle Prospektionen in Taljanky und Maydanetske (Ukraine) im Vergleich mit früheren Forschungen. In: W. Schier and F. Drașovean (eds.), The Neolithic and Eneolithic in Southeast Europe: New approaches to dating and cultural Dynamics in the 6th to 4th Millennium BC. Prähistorische Archäologie in Südosteuropa 28 (Rahden/Westf. 2014) 99–112.

Rassmann et al. 2014b: K. Rassmann, R. Ohlrau, R. Hofmann, C. Mischka, N. Burdo, M. Yu. Videjko, and J. Müller, High precision Tripolye settlement plans, demographic estimations and settlement organization. Journal of Neolithic Archaeology 16, 2014, 63–95 [doi 10.12766/jna.2014.3].

Reingruber 2024: A. Reingruber, The Oïkos, the Orygma and the Open Spaces: Aegean Neolithic Settlement Patterns in Perspective. In: T. Kienlin (ed.), Household Practices and Houses – Current Approaches from Archeology and the Sciences. Universitätsforschungen zur prähistorischen Archäologie 399 (Bonn 2024) 79–104.

Sarris et al. 2015: A. Sarris, C. C. Garcia, T. Kalayci, F.-X. Simon, G. Cantoro, J. Donati, M. Manataki, K. Vouzaxakis, V. Rondiri, P. Arachoviti, K. Almatzi, D. Efstratiou, and E. Stamelou, Magoula Visviki from a Geophysical Prospection Perspective. In: E. Alram-Stern und A. Dousougli-Zachos, Visviki-Magula / Velestino. Die neolithischen Befunde und Funde. Die Deutschen Ausgrabungen 1941. Beiträge zur ur- und frühgeschichtlichen Archäologie des Mittelmeer-Kulturraumes 36 (Bonn 2015) 573–579.

Sarris et al. 2017: A. Sarris, T. Kalayci, F.-X. Simon, J. Donati, C. Cuenca García, M. Manataki, G. Cantoro, I. Moffat, E. Kalogiropoulou, G. Karampatsou, K. Armstrong, N. Argyriou, S. Dederix, C. Manzetti, N. Nikas, K. Vouzaxakis, V. Rondiri, P. Arachoviti, K. Almatzi, D. Efstathiou, and E. Stamelou, Opening a New Frontier in the Study of Neolithic Settlement Patterns of Eastern Thessaly, Greece. In: A. Sarris, E. Kalogiropoulou, T. Kalayci, and L. Karimali (eds.), Communities, Landscapes and Interaction in Neolithic Greece. International Conference, Rethymno 29–30 May 2014. International Monographs in Prehistory, Archaeological Series 20 (Michigan 2017) 27–48.

Schenk and Goldmann 2003: T. Schenk and T. Goldmann, Die Seddiner Kultfeuerreihe. Geomagnetische Prospektion am Königsgrab in der Prignitz. Archäologie in Berlin und Brandenburg 2003, 2004, 57–59.

Theocharis 1973: D. R. Theocharis (ed.), Neolithic Greece (Athens 1973) 17–128.

Toufexis 2006: G. Toufexis, The Lake Karla (Viivis) and the excavation at the prehistoric settlement at Palioskala: First results and perspectives [in Greek]. In: A. Mazarakis Ainian (ed.), Archaeological Meeting of Thessaly and Central Greece 1. Ministry of Culture and the University of Thessaly, Volos, 27.2–2.3.2003 (Volos 2006) 55–70.

Toufexis 2017: G. Toufexis, Oikistiki drastiriotita kai organosi tou horou stous oikismous tis Neoteris Neolithikis sti Thessalia: Paradeigmata apo tous oikismous ston Profiti Ilia Mandras, Makrychori, Galene and Rachmani. PhD thesis, University of Thessaly (2017). http://hdl.handle.net/10442/hedi/41426

Tsokas 2006: G. Tsokas, Archaiologia & geophysikē: exereunōntas ton archaiologiko chōro tēs Berginas (1984–2004). Univ. Studio Press (Thessaloniki 2006).

Wijnen 1992: M.-H. Wijnen, Building Remains of the Early Neolithic Period at Sesklo. In: Διεθνές συνέδριο για την Αρχαία Θεσσαλία, στη μνήμη του Δ.Ρ. Θεοχάρη. Πρακτικά (Athens 1992) 55–63.